Published by
NIGERIAN SOCIETY OF PHYSICAL SCIENCES
Available online @ https://journal.nsps.org.ng/index.php/jnsps

J. Nig. Soc. Phys. Sci. 8 (2026) 2942

Journal of the Nigerian Society of Physical Sciences

Onchocerciasis control via Caputo-Fabrizio fractional dynamics: a focus on early treatment and vector management strategies

Danat Nanle Tanko[a,b], Farah Aini Abdullah[a,*], Majid K. M Ali[a], Matthew O. Adewole[a,c], James Andrawus[d]

[a]*School of Mathematical Sciences, Universiti Sains Malaysia, 11800 USM, Pulau Pinang, Malaysia*
[b]*Department of Mathematics, Plateau State University Bokkos, 2012 Jos, Plateau State, Nigeria*
[c]*Department of Computer Science and Mathematics, Mountain Top University, Prayer City, Ogun State, Nigeria*
[d]*Department of Mathematics, Federal University, Dutse 7156, Jigawa, Nigeria*

Abstract

The socio-economic burdens of onchocerciasis have prompted the formulation of several mathematical models to better comprehend the epidemic. However, existing models either use integer-order derivatives, which often do not capture the memory and non-local effects seen in infectious diseases, or fractional order with singularity kernels, which may inadequately represent memory effects due to their singularity kernels. Onchocerciasis has a prolonged incubation and slow progression, making past conditions impactful on the disease's current and future course. Fractional derivatives effectively capture this memory effect, providing a more realistic depiction of the infection dynamics than integer-order models. We propose a non-local, non-singular exponential kernel fractional-order onchocerciasis model in the Caputo-Fabrizio fractional derivative sense to capture the disease's memory effects. Our model incorporates early treatment of exposed individuals as a critical intervention parameter, and vector management strategies are also incorporated. Using fixed-point theorem and iterative methods, we establish the existence and uniqueness of solutions, derive conditions for onchocerciasis-free and endemic equilibrium points, and analyze their stability, confirming the model's biological feasibility. Numerical simulations are conducted using a three-step fractional Adams-Bashforth method. Sensitivity analyses indicate that vector management and early treatment effectively reduce the effective reproduction number, while increases in the human-to-vector contact rate elevate it. Numerical results demonstrate that early treatment and vector management can significantly control onchocerciasis. The fractional-order "memory effect" highlights the importance of continuous monitoring and consistent application of control measures to reduce the memory index and curb onchocerciasis prevalence over time.

DOI:10.46481/jnsps.2026.2942

Keywords: Caputo-Fabrizio fractional derivative, Existence, Stability, Fractional Adams-Bashforth Numerical scheme, Onchocerciasis model

Article History :
Received: 18 May 2025
Received in revised form: 14 July 2025
Accepted for publication: 29 September 2025
Available online: 31 October 2025

© 2025 The Author(s). Published by the Nigerian Society of Physical Sciences under the terms of the Creative Commons Attribution 4.0 International license. Further distribution of this work must maintain attribution to the author(s) and the published article's title, journal citation, and DOI.

Communicated by: Joel Ndam

1. Introduction

Onchocerciasis (river blindness) is a neglected tropical disease (NTD) with a significant socio-economic burden on affected communities [1].

*Corresponding author Tel. No.: +6-016-443-7864.
Email address: farahaini@usm.my (Farah Aini Abdullah)

The parasite *Onchocerca volvulus* causes the disease and is transmitted to humans through the bite of infected blackflies (*Simulium* species) during blood meals [2]. The flies thrive near fast-flowing rivers [3]. While onchocerciasis is most common in Africa, cases have also been reported in Yemen and Latin America [4, 5].

Once the parasite's larvae (microfilariae) are in humans, they develop into adult worms (macrofilariae) that release numerous microfilariae into the body. Ivermectin is the primary treatment, targeting microfilariae and halting their transmission [6–8]. However, no medications exist to eliminate adult macrofilariae [4, 8–10], leading to ongoing complications. The disease causes disfiguring skin changes (leopard and lizard skin) and eye damage.

Health intervention programs, such as the World Health Organization (WHO), the Onchocerciasis Elimination Program of the Americas (OEPA), the African Programme for Onchocerciasis Control (APOC), and the Onchocerciasis Control Programme in West Africa (OCP) [5, 11, 12], have had varying degrees of success in controlling the disease. Yet the disease persists with an estimated 37 million individuals infected worldwide. Among these, approximately 14.6 million suffer from skin disorders, over 270,000 are blind, and roughly 1.2 million experience visual impairment [10, 13, 14].

Several mathematical models based on integer-order differential equations (IODEs) have studied the dynamics of onchocerciasis [15–23]. Walker et al. [22] developed models to evaluate the feasibility of eliminating onchocerciasis through mass drug administration (MDA) with ivermectin and vector control strategies. The studies by Bas et al. [21] and Tirados et al. [23] did not incorporate vector control strategies, despite being a valuable complementary strategy when elimination through MDA alone is uncertain. While the model in Omondi et al. [16] asserted that MDA with ivermectin alone cannot eliminate the disease and highlighted the importance of timely treatment, Konlan et al. [18] emphasized that proper monitoring of human migration and vector control are critical to onchocerciasis elimination.

However, the "memory effects", genetic traits, and long-term interactions that govern a variety of phenomena (like the onchocerciasis dynamics) are not accounted for by the IODEs models [24]. Fractional-order differential equations (FODEs) models are valuable tools that overcome these limitations [25–27]. Studies show that FODE models yield better fitting results than IODE models [28, 29]. These models are gaining popularity in science because they forecast a system's future conditions by considering its present and prior states, a characteristic that IODE models cannot address [30, 31].

Several studies have utilized fractional operators to approximate solutions for real-world phenomena [32–35]. Specifically, infectious disease models using fractional operators are explored in Ref.[25, 36–39]. However, so far reviewed, very few studies have examined onchocerciasis dynamics using fractional derivatives; only the Caputo fractional derivative has been utilized [40, 41]. Atangana and Alqahtani's [40] study focuses on analytical and numerical approximation techniques using Homotopy Methods and emphasizes that incorporating memory (FODEs) enhances the design of effective, time-aware interventions. In contrast, Onifade et al. [41] suggest that environmental control strategies are essential for disease elimination. However, the Caputo derivative singularity kernel limits its applicability and effectiveness in appropriately representing the memory effect in real-life systems [30, 42, 43].

The Caputo-Fabrizio fractional derivative (CFFD), based on a non-singular kernel [44], addresses the Caputo limitation and has been used to model real-world phenomena [31, 45–48]. While no studies have yet applied the CFFD to model onchocerciasis dynamics, researchers have used it to model COVID-19 [25, 39], HIV/AIDS [49], dengue fever [50], and host-vector diseases [51].

Although onchocerciasis is curable at an early stage, previous models do not exclusively consider the impact of early treatment of exposed individuals as containment strategies, but rather MDA treatment. The representation of disease memory effects has been considered using fractional derivatives with singularity kernels.

This study formulates a Caputo-Fabrizio (CF) fractional mathematical model for onchocerciasis dynamics, integrating early treatment of exposed individuals and vector control as intervention strategies. We use CF memory effects to assess the impact of control strategies, as the disease leaves immunological and epidemiological memory in humans. Our goal is to provide insights on effectively controlling and eradicating onchocerciasis. The CF is chosen for exhibiting a non-singular exponential kernel, ensuring smoother, more stable numerical simulations and a fading memory [44].

The fractional 3-step Adam Bashforth numerical scheme was chosen for the model simulation due to its efficiency and better performance by reusing values from previous time steps, making it appropriate for fractional differential equations with memory effects [52, 53]. It has been utilized in an infectious disease model in the FC sense [49, 52–54].

In this study, Section 2 provides basic definitions of the CF derivative, Section 3 presents the description and formulation of the model, the model's properties are given in Section 4, Section 5 presents the determination of the model's equilibria, the numerical method and simulation are described in Section 6, the impact of memory effects is discussed in Section 7, and Section 8 concludes the study.

2. Basic definitions

The properties of the Caputo-Fabrizio derivative are outlined in Ref. [55]. We consider the following definitions for our model analysis.

Let $H^1(\upsilon_1, \upsilon_2)$ denote the set of all functions φ on the interval (υ_1, υ_2) such that both φ and φ' are in $L^2(\upsilon_1, \upsilon_2)$. Where (υ_1, υ_2) is the set of measurable functions on whose squares are Lebesgue-integrable, that is;

$$L^2(\upsilon_1, \upsilon_2) = \left\{ f : \int_{\upsilon_1}^{\upsilon_2} |f(\upsilon)|^2 \, d\upsilon < \infty \right\}.$$

Employing this definition of $H^1(\upsilon_1, \upsilon_2)$, we consider the following.

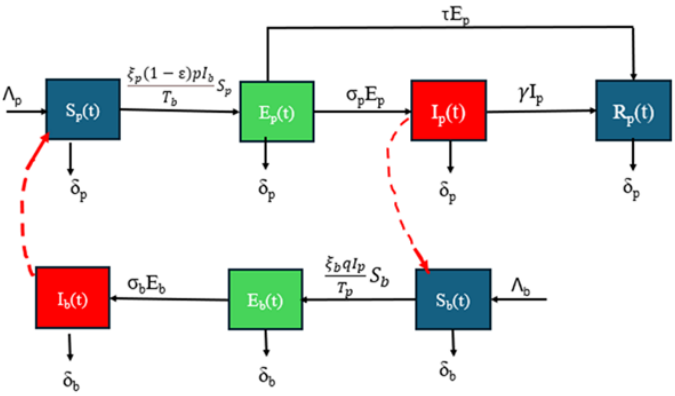

Figure 1. Schematic transmission dynamics of onchocerciasis

Definition 1. *As seen in Refs. ([44, 56, 57]). Let $\varphi \in H^1(\upsilon_1, \upsilon_2)$ and $\beta \in (0, 1)$. The CF derivative of the order β from υ_1 to t is defined as:*

$$ {}^{CF}_{\upsilon_1}D^{\beta}_{t}\varphi(t) = \frac{M(\beta)}{1-\beta}\int_{\upsilon_1}^{t}\varphi'(t)\exp\left[-\frac{\beta(t-\upsilon)}{1-\beta}\right]d\upsilon, \tag{1} $$

where $M(\beta)$ is consider as normalized constant(or function) satisfying $M(1) = M(0) = 1$. On the other hand, if $\varphi \notin H^1(\upsilon_1, \upsilon_2)$ then we have:

$$ {}^{CF}_{\upsilon_1}D^{\beta}_{t}\varphi(t) = \frac{\beta M(\beta)}{1-\beta}\int_{\upsilon_1}^{t}(\varphi(t)-\varphi(\upsilon))\exp\left[-\frac{\beta(t-\upsilon)}{1-\beta}\right]d\upsilon. \tag{2} $$

Definition 2. *As seen in Refs. ([56–58]). Let $\beta \in (0, 1)$ where β is the order of the integral. Then the CF integral of order β of a function φ, is defined by;*

$$ {}^{CF}I^{\beta}_{t}\varphi(t) = \frac{1-\beta}{M(\beta)}\varphi(t) + \frac{\beta}{M(\beta)}\int_{0}^{t}\varphi(\upsilon)d\upsilon, t \geq 0. \tag{3} $$

3. Description and formulation of the model

We developed a deterministic fractional-order mathematical model. Our model is based on the idea of the IODE model in Refs. [18–20], which examines the interaction between humans (persons) and black flies (vectors). Unlike our model, though simplified, the studies in Refs. [18–20] did not account for recovery compartment dynamics or the early treatment of exposed individuals.

At time $t \geq 0$, $T_p(t)$ and $T_b(t)$ represent the total populations of humans and vectors, respectively. $T_p(t)$ is divided into four compartments: susceptible persons $S_p(t)$ - those at risk of contracting onchocerciasis but not infected; exposed persons $E_p(t)$ - people exposed to onchocerciasis but not contagious; infected persons $I_p(t)$ - those currently infected and infectious; and recovered persons $R_p(t)$ - individuals who have recovered from onchocerciasis. Since onchocerciasis can be treated and eliminated at the microfilariae stage, we formulate the model to reflect recovery due to early treatment at rate τ, and recovery due to delayed treatment at rate γ.

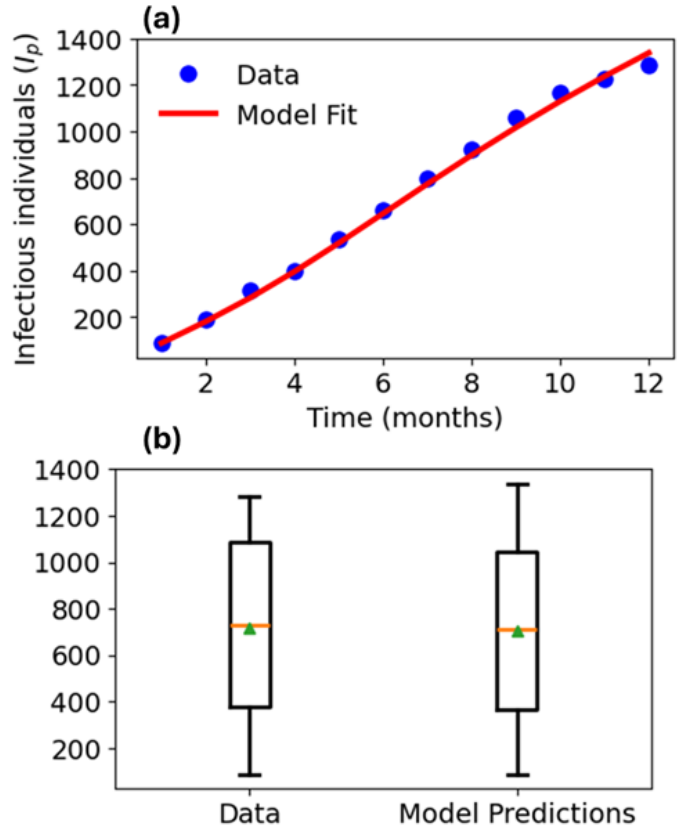

Figure 2. (a) Fitted comparison between the diseases' actual data and the simulations produced by the model (7) (b) Statistical illustration of actual data and model prediction using box and whisker plot.

The $T_b(t)$ is divided into three compartments: susceptible black flies $S_b(t)$ - those that have not encountered an infected human; exposed black flies $E_b(t)$ - those that have acquired microfilariae but do not transmit infection; and infectious black flies $I_b(t)$ - vectors that carry the infective larvae and are contagious.

The model assumes a constant recruitment rate Λ_p of $S_p(t)$ through immigration or birth, and they become infected through contact with infectious female black flies during blood meals. A fraction of $S_p(t)$ progresses to exposed persons $E_p(t)$ at a force infection rate ψ_p defined in Equation (4). The model assumes a constant recruitment rate Λ_p of $S_p(t)$ through immigration or birth, and they become infected through contact with infectious female black flies during blood meals. A fraction of $S_p(t)$ progresses to exposed persons $E_p(t)$ at a force infection rate ψ_p defined in Equation (4). Assuming the probability of transmitting the disease per bite of the infectious black fly to humans is at rate p $(0 \leq p \leq 1)$. The $E_p(t)$ is early treated and progresses to recovered persons $R_p(t)$ at a treatment rate τ. A fraction of the exposed persons who were not early treated become infectious persons $I_p(t)$ at rate σ_p. The $I_p(t)$ receive treatment at rate γ, and progress to recovered persons $R_p(t)$. Assuming the probability of transmitting the disease from infectious humans to black flies is at the biting rate q $(0 \leq q \leq 1)$. The model assumes a constant vector recruitment rate Λ_b of $S_b(t)$ through birth. A fraction of $S_b(t)$ progresses to exposed black flies $E_b(t)$

at a force of infection rate ψ_b (Equation (5)) through biting infectious humans. The $E_b(t)$ progress to infectious black flies $I_b(t)$ at rate σ_b. We assume a natural death rate δ_p and δ_b in all human and vector compartments, respectively.

We assume the effective contact of human-to-vector transmitting infection to humans is at the rate ξ_p, at the biting rate p, while the effective contact of vector-to-human transmitting infection to vectors is at the rate ξ_b, at the biting rate q. Hence, the force of infection ψ_p and ψ_b are defined as;

$$\psi_p = \frac{\xi_p p I_b(1-\varepsilon)}{T_b}. \tag{4}$$

$$\psi_b = \frac{\xi_b q I_p}{T_p}. \tag{5}$$

We incorporate vector control with the parameter ε, which includes strategies like applying repellent and wearing protective clothing during black-fly peak times. Insecticide spraying with larvicides and adulticides further reduces the vector population. We assumed $0 \le \varepsilon \le 1$; if vector control is 100% effective ($\varepsilon = 1$), and when no control is applied, $\varepsilon = 0$.

The model assumes constant recruitment of susceptible humans (via birth or immigration) and vector populations (via reproduction), and infected vectors do not live to recover from infection.

The system of classical differential Equations (6) with non-negative initial conditions represent the model equation.

$$\begin{aligned}
\frac{dS_p}{dt} &= \Lambda_p - \psi_p S_p - \delta_p S_p,\\
\frac{dE_p}{dt} &= \psi_p S_p - (\tau + \sigma_p + \delta_p)E_p,\\
\frac{dI_p}{dt} &= \sigma_p E_p - (\gamma + \delta_p)I_p,\\
\frac{dR_p}{dt} &= \tau E_p + \gamma I_p - \delta_p R_p,\\
\frac{dS_b}{dt} &= \Lambda_b - \psi_b S_b - \delta_b S_b,\\
\frac{dE_b}{dt} &= \psi_b S_b - (\sigma_b + \delta_b)E_b,\\
\frac{dI_b}{dt} &= \sigma_b E_b - \delta_b I_b.
\end{aligned} \tag{6}$$

The corresponding fractional model of Equation (6) in CF sense, as defined in Equation (1), yields:

$$\begin{aligned}
{}^{CF}D_t^{\beta} S_p(t) &= \Lambda_p - \psi_p S_p - \delta_p S_p,\\
{}^{CF}D_t^{\beta} E_p(t) &= \psi_p S_p - (\tau + \sigma_h + \delta_p)E_p,\\
{}^{CF}D_t^{\beta} I_p(t) &= \sigma_p E_p - (\gamma + \delta_p)I_p,\\
{}^{CF}D_t^{\beta} R_p(t) &= \tau E_p + \gamma I_p - \delta_p R_p,\\
{}^{CF}D_t^{\beta} S_b(t) &= \Lambda_b - \psi_b S_b - \delta_b S_b,\\
{}^{CF}D_t^{\beta} E_b(t) &= \psi_b S_b - (\sigma_b + \delta_b)E_b,\\
{}^{CF}D_t^{\beta} I_b(t) &= \sigma_b E_b - \delta_b I_b.
\end{aligned} \tag{7}$$

Table 1. Description of variables and parameters in model (7).

Variables	Description
T_p, T_b	Total human and vector populations.
S_p, S_b	Susceptible humans and vectors.
E_p, E_b	Exposed humans and vectors.
I_p, I_b	Infectious humans and vectors.
R_p	Recovered humans.
Parameters	**Description**
Λ_p, Λ_b	Human and vector Recruitment rates.
δ_p, δ_b	Human and vector mortality rates.
τ	Early Treatment rate.
ψ_p , ψ_b	Force of infection of humans and vectors.
ξ_p, ξ_b	Effective risk rate of humans and vectors.
σ_p ,σ_b	Progression rate of humans and vectors.
p	Transmission rate from vector to human.
q	Transmission rate from human to vector.
γ	Recovery rate of infectious humans.
ε	Vector control rate.

Subject to the initial conditions:

$$\begin{aligned}
S_p(0) = S_{p_0} > 0, E_p(0) = E_{p_0} \ge 0, I_p(0) = I_{p_0} \ge 0,\\
R_p(0) = R_{p_0} \ge 0,\\
S_b(0) = S_{b_0} > 0, E_b(0) = E_{b_0} \ge 0, I_b(0) = I_{b_0} \ge 0.
\end{aligned} \tag{8}$$

Table 1 describes the variables and parameters used to formulate the model equation.

4. Properties of the model

In the following subsections, we examine several key aspects of the model equations to assess their accuracy.

4.1. The existence and uniqueness of the model's solutions.

The existence of the model's solution is examined by applying the Caputo integral operator in Equation (3) to Equation (7), we obtain:

$$\begin{aligned}
S_p(t) - S_p(0) &= {}^{CF}I_t^{\beta}\left[\Lambda_p - \psi_p S_p - \delta_p S_p\right],\\
E_p(t) - E_p(0) &= {}^{CF}I_t^{\beta}\left[\psi_p S_p - (\tau + \sigma_p + \delta_p)E_p\right],\\
I_p(t) - I_p(0) &= {}^{CF}I_t^{\beta}\left[\sigma_p E_p - (\gamma + \delta_p)I_p\right],\\
R_p(t) - R_p(0) &= {}^{CF}I_t^{\beta}\left[\tau E_p + \gamma I_p - \delta_p R_p\right],\\
S_b(t) - S_b(0) &= {}^{CF}I_t^{\beta}\left[\Lambda_b - \psi_b S_b - \delta_b S_b\right],\\
E_b(t) - E_b(0) &= {}^{CF}I_t^{\beta}\left[\psi_b S_b - (\sigma_b + \delta_b)E_b\right],\\
I_b(t) - I_b(0) &= {}^{CF}I_t^{\beta}\left[\sigma_b E_b - \delta_b I_b\right].
\end{aligned} \tag{9}$$

For the sake of analytical ease of use, we define the following

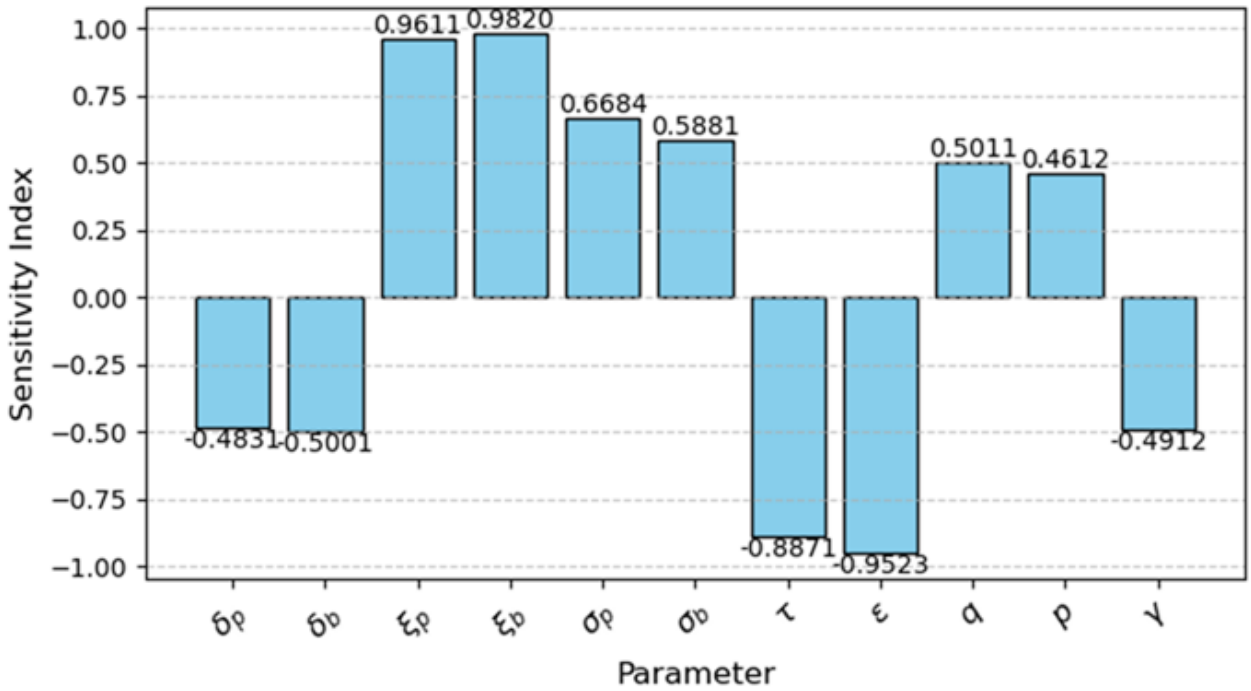

Figure 3. Sensitivity indices of $\mathcal{R}_c$.

kernels;

$$\begin{aligned}
K_1(t, S_p(t)) &= \Lambda_p - \psi_p S_p(t) - \delta_p S_p(t),\\
K_2(t, E_p(t)) &= \psi_p S_p(t) - (\tau + \sigma_p + \delta_p)E_p(t),\\
K_3(t, I_p(t)) &= \sigma_p E_p(t) - (\gamma + \delta_p)I_p(t),\\
K_4(t, R_p(t)) &= \tau E_p(t) + \gamma I_p(t) - \delta_p R_p(t),\\
K_5(t, S_b(t)) &= \Lambda_b - \psi_b S_b(t) - \delta_b S_b(t),\\
K_6(t, E_b(t)) &= \psi_b S_b(t) - (\sigma_b + \delta_b)E_b(t),\\
K_7(t, I_b(t)) &= \sigma_b E_b(t) - \delta_b I_b(t).
\end{aligned} \tag{10}$$

From Equation (3), let

$$\phi(\beta) = \frac{1-\beta}{M(\beta)}, \quad \psi(\beta) = \frac{\beta}{M(\beta)}. \tag{11}$$

We state the following theorem to establish that the kernels satisfy the Lipschitz and contraction criteria.

Theorem 1. *The kernels $K_i, i = 1, 2, ..., 7$ of the autonomous system (9) satisfy the Lipschitz conditions and are contraction mapping if the inequality holds*

$$\begin{aligned}
&0 \le L = \max\{\xi_1, \xi_2, \xi_3, \xi_4, \xi_5, \xi_6, \xi_7\} < 1,\\
&\text{and such that } \|K_i(t, \lambda) - K_i(t, \lambda_i)\| \le L\|\lambda - \lambda_i\|,
\end{aligned} \tag{12}$$

where λ and λ_i represent any two functions.

Proof. Assume that $S_p(t)$, $E_p(t)$, $I_p(t)$, $R_p(t)$, $S_b(t)$, $E_b(t)$, and $I_b(t)$ are nonnegative bounded functions and there exist $\omega_i > 0 (i = 1, 2, ..., 7)$ such that $\|S_p(t)\| \le \omega_1$, $\|E_p(t)\| \le \omega_2$, $\|I_p(t)\| \le \omega_3$, $\|R_p(t)\| \le \omega_4$, $\|S_b(t)\| \le \omega_5$, $\|E_b(t)\| \le \omega_6$, and $\|I_b(t)\| \le \omega_7$. Where $\|.\|$ denotes the maximum norms. For kernel K_1, let S_p and S_{1p} represent any two functions (with constant variables). Thus, we have:

$$\begin{aligned}
\|K_1(t, S_p) - K_1(t, S_{1p})\| &= \|-\psi_p(S_p(t) - S_{1p}(t))\\
&\quad - \delta_p(S_p(t) - S_{1p}(t))\|,\\
\|K_1(t, S_p) - K_1(t, S_{1p})\| &\le \|(\psi_p + \delta_p)(S_p(t) - S_{1p}(t))\|,\\
\|K_1(t, S_p) - K_1(t, S_{1p})\| &\le (\psi_p + \delta_p)\|(S_p(t) - S_{1p}(t))\|,\\
\|K_1(t, S_p) - K_1(t, S_{1p})\| &\le \xi_1\|(S_p(t) - S_{1p}(t))\|,
\end{aligned} \tag{13}$$

where $(\psi_p + \delta_p) = \xi_1 \in L < 1$. Similarly, results for the other kernels follow as;

$$\begin{aligned}
\|K_2(t, E_p) - K_2(t, E_{1p})\| &\le \xi_2\|(E_p(t) - E_{1p}(t))\|,\\
\|K_3(t, I_p) - K_3(t, I_{1p})\| &\le \xi_3\|(I_p(t) - I_{1p}(t))\|,\\
\|K_4(t, R_p) - K_4(t, R_{1p})\| &\le \xi_4\|(R_p(t) - R_{1p}(t))\|,\\
\|K_5(t, S_b) - K_5(t, S_{1b})\| &\le \xi_5\|(S_b(t) - S_{1b}(t))\|,\\
\|K_6(t, E_b) - K_6(t, E_{1b})\| &\le \xi_6\|(E_b(t) - E_{1b}(t))\|,\\
\|K_7(t, I_b) - K_7(t, I_{1b})\| &\le \xi_7\|(I_b(t) - I_{1b}(t))\|,
\end{aligned} \tag{14}$$

where all the ξ_i are given in Equation (15).

$$\begin{aligned}
&\xi_1 = \psi_p + \delta_p, \xi_2 = \tau + \sigma_p + \delta_p, \xi_3 = \gamma + \delta_p,\\
&\xi_4 = \delta_p, \xi_5 = \psi_b + \delta_b \xi_6 = \sigma_b + \delta_b, \xi_7 = \delta_b.
\end{aligned} \tag{15}$$

Thus, all the $K_i, i = 1, 2, ...7$ satisfied the Lipschitz condition and since $0 \le L = \max\{\xi_1, \xi_2, \xi_3, \xi_4, \xi_5, \xi_6, \xi_7\} < 1$, the kernels are contractions. The recursive formulas are introduced as follows: □

$$
\begin{aligned}
S_{p(n)}(t) &= K_1(t, S_{p(n-1)})\phi(\beta) + \psi(\beta)\int_0^t K_1(z, S_{p(n-1)})\,dz,\\
E_{p(n)}(t) &= K_2(t, E_{p(n-1)})\phi(\beta) + \psi(\beta)\int_0^t K_2(z, E_{p(n-1)})\,dz,\\
I_{p(n)}(t) &= K_3(t, I_{p(n-1)})\phi(\beta) + \psi(\beta)\int_0^t K_3(z, I_{p(n-1)})\,dz,\\
R_{p(n)}(t) &= K_4(t, R_{p(n-1)})\phi(\beta) + \psi(\beta)\int_0^t K_4(z, R_{p(n-1)})\,dz,
\end{aligned}
$$

$$
\begin{aligned}
S_{b(n)}(t) &= K_5(t, S_{b(n-1)})\phi(\beta) + \psi(\beta)\int_0^t K_5(z, S_{b(n-1)})\,dz,\\
E_{b(n)}(t) &= K_6(t, E_{b(n-1)})\phi(\beta) + \psi(\beta)\int_0^t K_6(z, E_{b(n-1)})\,dz,\\
I_{b(n)}(t) &= K_7(t, I_{b(n-1)})\phi(\beta) + \psi(\beta)\int_0^t K_7(z, I_{b(n-1)})\,dz,
\end{aligned}
\tag{16}
$$

with the following initial conditions;

$$
\begin{aligned}
S_{p(0)}(t) = S_p(0), E_{p(0)}(t) = E_p(0), I_{p(0)}(t) = I_p(0),\\
R_{p(0)}(t) = R_p(0), S_{b(0)}(t) = S_b(0), E_{b(0)}(t) = E_b(0),\\
I_{b(0)}(t) = I_b(0).
\end{aligned}
\tag{17}
$$

From Equation (16) the difference between consecutive approximations is given as:

$$
\begin{aligned}
\Omega_{1(n)}(t) &= \phi(\beta[K_1(t, S_{p(n-1)}) - K_1(t, S_{p(n-2)})]\\
&\quad + \psi(\beta)\int_0^t [K_1(z, S_{p(n-1)}) - K_1(z, S_{p(n-2)})]\,dz,\\
\Omega_{2(n)}(t) &= \phi(\beta)[K_2(t, E_{p(n-1)}) - K_2(t, E_{p(n-2)})]\\
&\quad + \psi(\beta)\int_0^t [K_2(z, E_{p(n-1)}) - K_2(z, E_{p(n-2)})]\,dz,\\
\Omega_{3(n)}(t) &= \phi(\beta)[K_3(t, I_{p(n-1)}) - K_3(t, I_{p(n-2)})]\\
&\quad + \psi(\beta)\int_0^t [K_3(z, I_{p(n-1)}) - K_3(z, I_{p(n-2)})]\,dz,\\
\Omega_{4(n)}(t) &= \phi(\beta)[K_4(t, R_{p(n-1)}) - K_4(t, R_{p(n-2)})]\\
&\quad + \psi(\beta)\int_0^t [K_4(z, R_{p(n-1)}) - K_4(z, R_{p(n-2)})]\,dz,\\
\Omega_{5(n)}(t) &= \phi(\beta)[K_5(t, S_{b(n-1)}) - K_5(t, S_{b(n-2)})]\\
&\quad + \psi(\beta)\int_0^t [K_5(z, S_{b(n-1)}) - K_5(z, S_{b(n-2)})]\,dz,\\
\Omega_{6(n)}(t) &= \phi(\beta)[K_6(t, E_{b(n-1)}) - K_6(t, E_{b(n-2)})]\\
&\quad + \psi(\beta)\int_0^t [K_6(z, E_{b(n-1)}) - K_6(z, E_{b(n-2)})]\,dz,\\
\Omega_{7(n)}(t) &= \phi(\beta)[K_7(t, I_{b(n-1)}) - K_7(t, I_{b(n-2)})]\\
&\quad + \psi(\beta)\int_0^t [K_7(z, I_{b(n-1)}) - K_7(z, I_{b(n-2)})]\,dz.
\end{aligned}
\tag{18}
$$

Note that,

$$
\begin{aligned}
S_{p(n)}(t) &= \sum_{i=1}^{n}\Omega_{1(i)}(t), E_{p(n)}(t) = \sum_{i=1}^{n}\Omega_{2(i)}(t),\\
I_{p(n)}(t) &= \sum_{i=1}^{n}\Omega_{3(i)}(t), R_{p(n)}(t) = \sum_{i=1}^{n}\Omega_{4(i)}(t),\\
S_{b(n)}(t) &= \sum_{i=1}^{n}\Omega_{5(i)}(t), E_{b(n)}(t) = \sum_{i=1}^{n}\Omega_{6(i)}(t),\\
I_{b(n)}(t) &= \sum_{i=1}^{n}\Omega_{7(i)}(t).
\end{aligned}
\tag{19}
$$

Equation (19) is valid because each term of $S_{p(n)}(t), E_{p(n)}(t), I_{p(n)}(t), ..., I_{b(n)}(t)$ is constructed iteratively from the differences $\Omega_{1(i)}(t), \Omega_{2(i)}(t), \Omega_{3(i)}(t), ..., \Omega_{7(i)}(t)$ that indicates how much the approximation changes at each step. From Equation (18), recursive inequalities are formulated for the differences $\Omega_{1(i)}(t)$, $\Omega_{2(i)}(t)$, $\Omega_{3(i)}(t)$, $\Omega_{4(i)}(t)$, $\Omega_{5(i)}(t)$, $\Omega_{6(i)}(t)$ and $\Omega_{7(i)}(t)$, as follows;

$$
\begin{aligned}
\|\Omega_{1(n)}(t)\| &= \|S_{p(n)}(t) - S_{p(n-1)}(t)\|\\
&\le \phi(\beta)\left\|K_1(t, S_{p(n)}) - K_1(t, S_{p(n-1)})\right\|\\
&\quad + \psi(\beta)\int_0^t \left\|K_1(z, S_{p(n)}) - K_1(z, S_{p(n-1)})\right\|\,dz
\end{aligned}
\tag{20}
$$

Since K_1 satisfies the Lipschitz condition with the Lipschitz constant, we have:

$$
\|\Omega_{1(n)}(t)\| \le \phi(\beta)\xi_1\|\Omega_{1(n-1)}(t)\| + \psi(\beta)\xi_1\int_0^t \|\Omega_{1(n-1)}(z)\|\,dz. \tag{21}
$$

Similarly, we have the following results;

$$
\begin{aligned}
\|\Omega_{2(n)}(t)\| &\le \phi(\beta)\xi_2\|\Omega_{2(n-1)}(t)\| + \psi(\beta)\xi_2\int_0^t \|\Omega_{2(n-1)}(z)\|\,dz,\\
\|\Omega_{3(n)}(t)\| &\le \phi(\beta)\xi_3\|\Omega_{3(n-1)}(t)\| + \psi(\beta)\xi_3\int_0^t \|\Omega_{3(n-1)}(z)\|\,dz,\\
\|\Omega_{4(n)}(t)\| &\le \phi(\beta)\xi_4\|\Omega_{4(n-1)}(t)\| + \psi(\beta)\xi_4\int_0^t \|\Omega_{4(n-1)}(z)\|\,dz,\\
\|\Omega_{5(n)}(t)\| &\le \phi(\beta)\xi_5\|\Omega_{5(n-1)}(t)\| + \psi(\beta)\xi_5\int_0^t \|\Omega_{5(n-1)}(z)\|\,dz,\\
\|\Omega_{6(n)}(t)\| &\le \phi(\beta)\xi_6\|\Omega_{6(n-1)}(t)\| + \psi(\beta)\xi_6\int_0^t \|\Omega_{6(n-1)}(z)\|\,dz,\\
\|\Omega_{7(n)}(t)\| &\le \phi(\beta)\xi_7\|\Omega_{7(n-1)}(t)\| + \psi(\beta)\xi_7\int_0^t \|\Omega_{7(n-1)}(z)\|\,dz.
\end{aligned}
$$

Below we consider the theorem, which guarantees the existence of a solution to model (7) - (8).

Theorem 2. *A set of solutions for onchocerciasis model (7) - (8) exists if time $t_0 > 0$ such that the following relation holds*

$$
\phi(\beta)\xi_i + \psi(\beta)\xi_i t_0 < 1 \quad \text{for } i = 1, 2, \ldots, 7. \tag{22}
$$

Proof. Since we assume that the function $S_p(t), E_p(t), I_p(t), R_p(t), S_b(t), E_b(t)$ and $I_b(t)$ are bounded, and that each of the kernels satisfied Lipschitz conditions, we obtained the following using Equations (21) recursively. For some $n-1$, the following inequality holds.

$$\|\Omega_{1(n-1)}(t)\| \leq \|S_p(0)\|[\phi(\beta)\xi_1 + \psi(\beta)\xi_1 t]^{n-1}. \tag{23}$$

Substitute Equation (23) into Equation (21)), we have:

$$\|\Omega_{1(n)}(t)\| \leq \xi_1\|S_p(0)\|\Big\{\phi(\beta)\,[W_1]^{n-1} + \psi(\beta_1)\int_0^t [W_2]^{n-1}\,dz\Big\}, \tag{24}$$

where $W_1 = \phi(\beta)\xi_1 + \psi(\beta)\xi_1 t$, $W_2 = \phi(\beta)\xi_1 + \psi(\beta)\xi_1 z$. Approximate the integral term using a linear bound since the power of the expression is dependent on z. We assume the integral is bounded by considering the maximum value over the interval $[0, t]$.

$$\int_0^t [\phi(\beta)\xi_1 + \psi(\beta)\xi_1 z]^{n-1}\,dz \leq t\cdot[W_1]^{n-1}. \tag{25}$$

Substitute (25) into (24), and simplify gives

$$\|\Omega_{1(n)}(t)\| \leq \|S_p(0)\|[\phi(\beta)\xi_1 + \psi(\beta)\xi_1 t]^{n}. \tag{26}$$

Similarly, we obtained the following:

$$\begin{aligned}
\|\Omega_{2(n)}(t)\| &\leq \|E_p(0)\|[\phi(\beta)\xi_2 + \psi(\beta)\xi_2 t]^{n},\\
\|\Omega_{3(n)}(t)\| &\leq \|I_p(0)\|[\phi(\beta)\xi_3 + \psi(\beta)\xi_3 t]^{n},\\
\|\Omega_{4(n)}(t)\| &\leq \|R_p(0)\|[\phi(\beta)\xi_4 + \psi(\beta)\xi_4 t]^{n},\\
\|\Omega_{5(n)}(t)\| &\leq \|S_b(0)\|[\phi(\beta)\xi_5 + \psi(\beta)\xi_5 t]^{n},\\
\|\Omega_{6(n)}(t)\| &\leq \|E_b(0)\|[\phi(\beta)\xi_6 + \psi(\beta)\xi_6 t]^{n},\\
\|\Omega_{7(n)}(t)\| &\leq \|I_b(0)\|[\phi(\beta)\xi_7 + \psi(\beta)\xi_7 t]^{n}.
\end{aligned} \tag{27}$$

Equations (26) and (27) show the existence of the solution. Furthermore, the function $S_p(t), E_p(t), I_p(t), R_p(t), S_b(t), E_b(t)$ and $I_b(t)$ need to converges to the system of Equations (7) - (8). We denote $H_n(t), I_n(t), J_n(t), K_n(t), L_n(t), M_n(t)$ and $N_n(t)$ as the remainder terms after n iterations.
$H_n(t)$ is defined as the difference between the exact solution (true state) $S_p(t)$ and the approximate solution (recursive approximation) $S_{p(n)}(t)$ expressed as:

$$H_n(t) = \phi(\beta_1)\Big[K_1(t, S_p) - K_1(t, S_{p(n-1)})\Big] + \psi(\beta_1)\int_0^t \Big[K_1(z, S_p) - K_1(z, S_{p(n-1)})\Big]\,dz. \tag{28}$$

The exact solution of the error term definition of $H_n(t)$ is

$$S_p(t) - S_p(0) = S_{p(n)}(t) - H_n(t). \tag{29}$$

Similarly, we obtained the following;

$$\begin{aligned}
E_p(t) - E_p(0) &= E_{p(n)}(t) - I_n(t),\\
I_p(t) - I_p(0) &= I_{p(n)}(t) - J_n(t),\\
R_p(t) - R_p(0) &= R_{p(n)}(t) - K_n(t),\\
S_b(t) - S_b(0) &= S_{b(n)}(t) - L_n(t),\\
E_b(t) - E_b(0) &= E_{b(n)}(t) - M_n(t),\\
I_b(t) - I_b(0) &= I_{b(n)}(t) - N_n(t).
\end{aligned} \tag{30}$$

Applying the Lipschitz criterion and the triangular inequality to the kernel K_1 on Equation (28), we get;

$$\|H_n(t)\| \leq \phi(\beta)\Big\|K_1(t, S_p) - K_1(t, S_{h(n-1)})\Big\| + \psi(\beta)\int_0^t \Big\|K_1(z, S_p) - K_1(z, S_{p(n-1)})\Big\|.dz. \tag{31}$$

Since the kernel K_1 function satisfies the Lipschitz condition, we have:

$$\|H_n(t)\| \leq \phi(\beta)\xi_1\|S_p(t) - S_{p(n-1)}(t)\| + \psi(\beta)\xi_1\int_0^t \|S_p(t) - S_{p(n-1)}(t)\|\,dz$$

From Equation (29), $S_p(t) - S_{p(n-1)}(0) = H_{(n-1)}(t)$. Thus,

$$\|H_n(t)\| \leq \phi(\beta)\xi_1\|H_{n-1}(t)\| + \psi(\beta)\xi_1\int_0^t \|H_{n-1}(z)\|\,dz$$

We assume inductively that the previous error term satisfies:

$$\|H_{n-1}(t)\| \leq [(\phi(\beta) + \psi(\beta)t_0)\,\xi_1]^{n},$$

and substitute this into $H_n(t)$ and factorized, we have;

$$\|H_n(t)\| \leq [(\phi(\beta) + \psi(\beta)t_0)\,\xi_1]^{n+1}. \tag{32}$$

Similarly, we have the following:

$$\begin{aligned}
\|I_n(t)\| &\leq [(\phi(\beta) + \psi(\beta)t_0)\,\xi_2]^{n+1},\\
\|J_n(t)\| &\leq [(\phi(\beta) + \psi(\beta)t_0)\,\xi_3]^{n+1},\\
\|K_n(t)\| &\leq [(\phi(\beta) + \psi(\beta)t_0)\,\xi_4]^{n+1},\\
\|L_n(t)\| &\leq [(\phi(\beta) + \psi(\beta)t_0)\,\xi_5]^{n+1},\\
\|M_n(t)\| &\leq [(\phi(\beta) + \psi(\beta)t_0)\,\xi_6]^{n+1},\\
\|N_n(t)\| &\leq [(\phi(\beta) + \psi(\beta)t_0)\,\xi_7]^{n+1}.
\end{aligned} \tag{33}$$

The limit of Equations (32) and (33) as n approaches infinity and with condition (22), gives $\|H_n(t)\| \to 0$, $\|I_n(t)\| \to 0$, $\|J_n(t)\| \to 0$, $\|K_n(t)\| \to 0$, $\|L_n(t)\| \to 0$, $\|M_n(t)\| \to 0$, and $\|N_n(t)\| \to 0$. Hence, the solution to the system (7) - (8) exists. □

The following theorem established the uniqueness of the solution.

Theorem 3. *The model (7) with its initial condition (8) has a unique set of solutions if the following conditions hold*

$$\phi(\beta)\xi_i + \psi(\beta)\xi_i t < 1 \quad \text{for } i = 1, 2, 3, \ldots, 7. \tag{34}$$

Proof. Suppose (34) holds, as proven by Theorem 1, assume there exists another set of solutions ($S_{1p}(t)$, $E_{1p}(t)$, $I_{1p}(t)$, $R_{1p}(t)$, $S_{1b}(t)$, $E_{1b}(t)$ and $I_{1b}(t)$) of the model other than ($S_p(t), E_p(t), I_p(t), R_p(t), S_b(t), E_b(t)$ and $I_b(t)$). Thus;

$$S_p(t) - S_{1p}(t) = \phi(\beta)\Big[K_1(t, S_p) - K_1(t, S_{1p})\Big] + \psi(\beta)\int_0^t \Big[K_1(z, S_p) - K_1(z, S_{1p})\Big]\,dz. \tag{35}$$

Applying the norm $\|.\|$ and triangle inequality to bothsides Equation (35) we have:

$$\|S_p(t) - S_{1p}(t)\| \leq \phi(\beta)\|K_1(t, S_p) - K_1(t, S_{1p})\| + \psi(\beta)\int_0^t \|K_1(z, S_p) - K_1(z, S_{1p})\|dz.$$

Applying Lipchitz condition on kernel K_1, we obtain;

$$\|S_p(t) - S_{1p}(t)\| \leq \phi(\beta)\xi_1\|S_p(t) - S_{1p}(t)\| + \psi(\beta)\xi_1 t\|S_p(t) - S_{1p}(t)\| \tag{36}$$

$$\|S_p(t) - S_{1p}(t)\| \leq (\phi(\beta)\xi_1 + \psi(\beta)\xi_1 t)\|S_p(t) - S_{1p}(t)\|.$$

From equation (36), we have;

$$\|S_p(t) - S_{1p}(t)\|(1 - \phi(\beta)\xi_1 - \psi(\beta)\xi_1 t) \leq 0. \tag{37}$$

$$\|S_p(t) - S_{1p}(t)\| \leq 0. \tag{38}$$

Equation (38), implies $S_p(t) = S_{1p}(t)$. Similarly applying the same procedure on each pair $\{E_p(t), E_{1p}(t)\}$, $\{I_p(t), I_{1p}(t)\}$, $\{R_p(t), R_{1p}(t)\}$, $\{S_b(t), S_{1b}(t)\}$, $\{E_b(t), E_{1b}(t)\}$,and $\{I_b(t), I_{1b}(t)\}$, we have;

$$\begin{aligned} &E_p(t) = E_{1p}(t), I_p(t) = I_{1p}(t), R_p(t) = R_{1p}(t), \\ &S_b(t) = S_{1b}(t), E_b(t) = E_{1b}(t), I_b(t) = I_{1b}(t). \end{aligned} \tag{39}$$

Thus, the theorem is proved. □

4.2. Positivity and boundedness of solution.

To ensure this in our model, we establish that all state variables remain non-negative for any time $t > 0$. Consequently, model (7) yields;

$$\begin{aligned} {}^{CF}D_t^{\beta} S_p(t)|_{S_p=0} &= \Lambda_p \gg 0, \\ {}^{CF}D_t^{\beta} E_p(t)|_{E_p=0} &= \psi_p S_p \geq 0, \\ {}^{CF}D_t^{\beta} I_p(t)|_{I_p=0} &= \sigma_p E_p \geq 0, \\ {}^{CF}D_t^{\beta} R_p(t)|_{R_p=0} &= \tau E_p + \gamma I_p \geq 0, \\ {}^{CF}D_t^{\beta} S_b(t)|_{S_b=0} &= \Lambda_b \gg 0, \\ {}^{CF}D_t^{\beta} E_b(t)|_{E_b=0} &= \psi_b S_b \geq 0, \\ {}^{CF}D_t^{\beta} I_b(t)|_{I_b=0} &= \sigma_b E_b \geq 0. \end{aligned} \tag{40}$$

Equation (40) shows that the model (7) is positive.

Theorem 4. *Assume that Ω is a biologically viable region provided for the model (7),then;*

$$\Omega = \left\{(S_p(t), E_p(t), I_p(t), R_p(t), S_b(t), E_b(t), I_b(t)) \in \mathbb{R}_+^7 : T_p \leq \frac{\Lambda_p}{\delta_p}, \quad T_b \leq \frac{\Lambda_b}{\delta_b}\right\}. \tag{41}$$

The positively invariant region Ω attracts all non-negative solutions for the model (7).

Proof. Our primary goal is to show that every solution in Ω stays in Ω. Therefore, considering the total human population of humans: $T_p(t) = S_p(t) + E_p(t) + I_p(t) + R_p(t)$. The derivative of $T_p(t)$ yields;

$${}^{CF}D_t^{\beta} T_p(t) \leq \Lambda_p - \delta_p T_p(t). \tag{42}$$

Equation (42) is solved in Caputo Fabrizio's sense, and we have the Laplace transformed solution as;

$$\frac{sT_p(s) - T_p(0)}{s(1-\beta) + \beta} \leq \frac{\Lambda_p}{s} + \delta_p T_p(s). \tag{43}$$

Taking the Laplace inverse, we have;

$$T_p(t) \leq \frac{\Lambda_p}{\delta_p} + \left[\frac{\Lambda_p(1-\beta) + T_p(0)}{1 + \delta_p(1-\beta)} - \frac{\Lambda_p}{\delta_p}\right] e^{\frac{-\delta_p \beta}{1+\delta_p(1-\beta)}t}. \tag{44}$$

Similarly, $T_b(t) = S_b(t) + E_b(t) + I_b(t)$ is the total population of blackflies, solving we have;

$$T_b(t) \leq \frac{\Lambda_b}{\delta_b} + \left[\frac{\Lambda_b(1-\beta) + T_b(0)}{1 + \delta_b(1-\beta)} - \frac{\Lambda_b}{\delta_b}\right] e^{\frac{-\delta_b \beta}{1+\delta_b(1-\beta)}t}. \tag{45}$$

From (44) and (45), we may now infer that $t \to 0$, $T_p(t) \to T_p(0) \implies T_p(t) \leq \frac{\Lambda_p}{\delta_p}$, and $T_b(t) \to T_b(0) \implies T_b(t) \leq \frac{\Lambda_b}{\delta_b}$. Consequently, Ω is a global attractor of all positive system solutions and positively invariant for arbitrary positive initial conditions. □

5. Existence of the model equilibria

At equilibrium, the rate of change of model (7) is set to be zero [39, 59]. Solving the resulting algebraic system for the state variables in terms of ψ_p and ψ_b, we obtained onchocerciasis-free and endemic equilibrium points.

5.1. Onchocerciasis-Free Equilibrium (OFE) points and determination of basic reproduction number

At OFE points, onchocerciasis transmission halts as there are no carriers to spread the pathogen. We denote $E^0 = (S_p^0, E_p^0, I_p^0, R_p^0, S_b^0, E_b^0, I_b^0)$ to be the onchocerciasis-free equilibrium point of the model. The stability of this equilibrium depends critically on the basic reproduction number (R_0), which determines whether the disease can re-establish itself after being introduced. Thus, the model (7) possesses a disease-free equilibrium as;

$$E^0 = \left(\frac{\Lambda_p}{\delta_p}, 0, 0, 0, \frac{\Lambda_b}{\delta_b}, 0, 0\right). \tag{46}$$

The number of new infections caused by onchocerciasis-infected individuals when they interact with the fully susceptible population in the absence of treatment and vector management is known as the basic reproduction number R_0, in our model (7).

Below, we calculate the basic reproduction number, which is obtained using the next-generation matrix method [60, 61]. To achieve the calculation of R_0 , we identify the disease class of the model (7) as done in [39] and denote such as

$D = \left[{}^{CF}D_t^{\beta_2}E_p,\ {}^{CF}D_t^{\beta_3}I_p,\ {}^{CF}D_t^{\beta_6}E_b,\ {}^{CF}D_t^{\beta_7}I_b\right]^T$ and splitting D into new infectious denoted by $f = \left[\psi_p S_p,\ 0,\ \psi_b S_b,\ 0\right]^T$ and transition infections denoted by $v = [(\tau+\sigma_p+\delta_p)E_p, -\sigma_p E_p+(\gamma+\delta_p)I_p,\ (\sigma_b+\delta_b)E_b,\ -\sigma_b E_b+\delta_b I_b]^T$. The basic reproduction R_0 is determined using the expression, $R_0 = \rho\left[\eta\ell^{-1}\right]$, where ρ is the spectral radius of the next-generation matrix $G_n = \eta\ell^{-1}$, η is the Jacobian matrix of new infections f and ℓ is the Jacobian matrix of transition infections v and are given below.

$$\eta = \begin{bmatrix} 0 & 0 & 0 & \frac{\xi_p(1-\epsilon)pS_p}{T_b} \\ 0 & 0 & 0 & 0 \\ 0 & \frac{\xi_b q S_b}{T_p} & 0 & 0 \\ 0 & 0 & 0 & 0 \end{bmatrix},$$
$$\ell = \begin{bmatrix} k_1 & 0 & 0 & 0 \\ -\sigma_p & k_2 & 0 & 0 \\ 0 & 0 & k_3 & 0 \\ 0 & 0 & -\sigma_b & \delta_b \end{bmatrix}. \tag{47}$$

The inverse of ℓ and the next-generation matrix denoted by $G_n = \eta\ell^{-1}$, are calculated and given as;

$$\ell^{-1} = \begin{bmatrix} \frac{1}{k_1} & 0 & 0 & 0 \\ \frac{\sigma_p}{k_1 k_2} & \frac{1}{k_2} & 0 & 0 \\ 0 & 0 & \frac{1}{k_3} & 0 \\ 0 & 0 & \frac{\sigma_b}{\delta_b k_3} & \frac{1}{\delta_b} \end{bmatrix},$$
$$G_n = \begin{bmatrix} 0 & 0 & \frac{\xi_p(1-\epsilon)p\sigma_p S_p}{k_3 T_b \delta_b} & \frac{\xi_p(1-\epsilon)pS_p}{T_b\delta_b} \\ 0 & 0 & 0 & 0 \\ \frac{\xi_b q\sigma_p S_p}{k_1 k_2 T_p} & \frac{\xi_b q S_b}{k_2 T_b} & 0 & 0 \\ 0 & 0 & 0 & 0 \end{bmatrix}. \tag{48}$$

The eigenvalues ($\lambda_i, i = 1,2,3,4$) of the G_n matrix is computed using $\det(\lambda I - G_n) = 0$ and yields:

$$[\lambda_1, \lambda_2, \lambda_3, \lambda_4]^T = \left[0, 0, \pm\sqrt{\frac{\xi_p\xi_b(1-\epsilon)pq\sigma_b\sigma_p}{k_1k_2k_3\delta_b}}\right]^T. \tag{49}$$

The effective reproduction number $\mathcal{R}_c$ is obtained by getting the dominant eigenvalues. The basic reproduction number R_0 can be calculated by setting all the control parameters in $\mathcal{R}_c$ to zero, that is ($\epsilon = \tau = 0$), thus, we have:

$$\mathcal{R}_c = \sqrt{\frac{\xi_p\xi_b(1-\epsilon)pq\sigma_b\sigma_p}{k_1k_2k_3\delta_b}},$$
$$R_0 = \sqrt{\frac{\xi_p\xi_b pq\sigma_b\sigma_p}{(\delta_p+\sigma_p)(\gamma+\delta_p)(\sigma_b+\delta_b)\delta_b}}. \tag{50}$$

Where $k_1 = \delta_p + \tau + \sigma_p, k_2 = \gamma + \delta_p, k_3 = \sigma_b + \delta_b$. The R_0 can be structurally simplified as:

$$R_0 = \sqrt{\frac{\text{(infection per bite)} \times \text{(progression rates)}}{\text{(removal rates)}}}.$$

From R_0 and R_c, sustained controls can eliminate onchocerciasis if $R_0 > 1$ but $R_c < 1$. If $R_0 < 1$, the disease may die out even without intervention; however, this outcome is unlikely for a burdensome disease such as onchocerciasis. Therefore, we base our subsequent analysis on R_c.

5.1.1. Local stability of onchocerciasis-free equilibrium

Here, for stability analysis, we consider the fractional-order linear system (52) with Caputo-Fabrizio derivative [62]. The fractional-order linear system has been used in similar infectious models [39, 49], for such analysis.

$${}^{CF}D_t^{\beta}x(t) = Bx(t), \tag{51}$$

where $x(t) \in \mathbb{R}^n$, $B \in \mathbb{R}^{n\times n}$ and $0 < \beta < 1$. Consequently, consider the definition and theorem.

Definition 3. *([62]). System (51) characteristic equation is described as;*

$$\det\left(s\left(I - (1-\beta)B\right) - \beta B\right) = 0. \tag{52}$$

Lemma 1. *The system given by Equation (52) is asymptotically stable if the real parts of the roots of its characteristic equation are negative, and the matrix $(I - (1-\beta)B)$ is invertible.*

Theorem 5. *If the real parts of the roots of the characteristic equation (53) are negative, then the onchocerciasis-free equilibrium point (E^0) of the model (7) with order β (where $0 < \beta < 1$) is locally asymptotically stable.*

$$\det\left(s\left(I - (1-\beta)J(E^0)\right) - \beta J(E^0)\right) = 0, \tag{53}$$

where $J(E^0) = B$ is the linearized matrix of the system (7) evaluated at the disease-free equilibrium points. We determine the linearized system of the model (7) at the onchocerciasis-free equilibrium (OFEP) as done in the infectious disease model [63, 64].

$$J(E^0) = \begin{bmatrix} -\delta_p & 0 & 0 & 0 & 0 & 0 & -\phi_1 \\ 0 & -k_1 & 0 & 0 & 0 & 0 & \phi_1 \\ 0 & \sigma_p & -k_2 & 0 & 0 & 0 & 0 \\ 0 & \tau & \gamma & -\delta_p & 0 & 0 & 0 \\ 0 & 0 & 0 & -\phi_2 & -\delta_b & 0 & 0 \\ 0 & 0 & 0 & \phi_2 & 0 & -k_3 & 0 \\ 0 & 0 & 0 & 0 & 0 & \sigma_b & -\delta_b \end{bmatrix}, \tag{54}$$

where $\phi_1 = \frac{\xi_p(1-\epsilon)pS_p^0}{T_b^0}$ and $\phi_2 = \frac{\xi_b q S_b^0}{T_p^0}$. Next, we established the invertibility of the matrix $\left(I - (1-\beta)J(E^0)\right)$ and the roots of (53). Let $M = \left(I - (1-\beta)J(E^0)\right)$, if the determinant $|M| \neq 0$ then M is invertible.

$$M = \begin{bmatrix} z_1 & 0 & 0 & 0 & 0 & 0 & l_7 \\ 0 & z_2 & 0 & 0 & 0 & 0 & l_8 \\ 0 & l_1 & z_3 & 0 & 0 & 0 & 0 \\ 0 & l_2 & l_3 & z_4 & 0 & 0 & 0 \\ 0 & 0 & 0 & l_4 & z_5 & 0 & 0 \\ 0 & 0 & 0 & l_5 & 0 & z_6 & 0 \\ 0 & 0 & 0 & 0 & 0 & l_6 & z_7 \end{bmatrix}.$$

where $z_1 = 1-(\beta-1)\delta_p, z_2 = 1-(\beta-1)k_1, z_3 = 1-(\beta-1)k_2, z_4 = 1-(\beta-1)\delta_p, z_5 = 1-(\beta-1)\delta_b, z_6 = 1-(\beta-1)k_3, z_7 = 1-(\beta-1)\delta_b, l_1 = (\beta-1)\sigma_p, l_2 = (\beta-1)\tau, l_3 = (\beta-1)\gamma, l_4 = (1-\beta)\phi_2, l_5 = (\beta-1)\phi_2, l_6 = (\beta-1)\sigma_b, l_7 = (1-\beta)\phi_1, l_8 = (\beta-1)\phi_1$.

$$|M| = z_1z_2z_3z_4z_5z_6z_7 - \phi_1\phi_2\sigma_p\sigma_b z_1z_4z_5\beta^4 + 4\phi_1\phi_2\sigma_p\sigma_b z_1z_4z_5\beta^3 - 6\phi_1\phi_2\sigma_p\sigma_b z_1z_4z_5\beta^2 + 4\phi_1\phi_2\sigma_p\sigma_b z_1z_4z_5\beta - \phi_1\phi_2\sigma_p\sigma_b z_1z_4z_5z_6.$$

$$|M| = \prod_{i=1}^{7} z_i - z_1 z_4 z_5 z_6 \phi_1 \phi_2 \sigma_p \sigma_b (\beta^4 - 4\beta^3 + 6\beta^2 - 4\beta + 1) \neq 0. \tag{55}$$

For $0 < \beta < 1$, $|M| \neq 0$, this implies that $\left(I - (1-\beta)J(E^0)\right)$ is invertible. Next, we compute the root of $\det\left(s\left(I - (1-\beta)J(E^0)\right) - \beta J(E^0)\right) = 0$. Let $N = \left(s\left(I - (1-\beta)J(E^0)\right) - \beta J(E^0)\right) = 0$

$$N = \begin{bmatrix} X_1 & 0 & 0 & 0 & 0 & 0 & A_7 \\ 0 & X_2 & 0 & 0 & 0 & 0 & A_8 \\ 0 & A_1 & X_3 & 0 & 0 & 0 & 0 \\ 0 & A_2 & A_3 & X_4 & 0 & 0 & 0 \\ 0 & 0 & A_4 & 0 & X_5 & 0 & 0 \\ 0 & 0 & A_5 & 0 & 0 & X_6 & 0 \\ 0 & 0 & 0 & 0 & 0 & A_6 & X_7 \end{bmatrix},$$

where $X_1 = sz_1 + \beta\delta_p, X_2 = sz_2 + k_1\beta, X_3 = sz_3 + k_2\beta, X_4 = sz_4 + \beta\delta_p, X_5 = sz_5 + \beta\delta_p, X_6 = sz_6 + \beta k_3, X_7 sz_7 + \beta\delta_p$, $A_1 = s(\beta-1)\sigma_p - \beta\sigma_p$, $A_2 = s(\beta-1)\tau - \beta\tau$, $A_3 = s(\beta-1)\gamma - \beta\gamma$, $A_4 = s(1-\beta)\phi_2 + \beta\phi_2$, $A_5 = s(\beta-1)\phi_2 - \beta\phi_2$, $A_6 = s(\beta-1)\sigma_b - \beta\sigma_b$, $A_7 = s(1-\beta)\phi_1 + \beta\phi_1$, $A_8 = s(\beta-1)\phi_1 - \beta\phi_1$.

$$|N| = (sz_1 + \beta\delta_p)(sz_2 + \beta k_1)(sz_3 + \beta k_2)(sz_4 + \beta\delta_p)(sz_5 + \beta\delta_b)(sz_6 + \beta k_3)(sz_7 + \beta\delta_b).$$

For $|N| = 0$ we have the following roots:

$$s_1 = -\frac{\beta}{z_1}\delta_p, s_2 = -\frac{\beta}{z_2}k_1, s_3 = -\frac{\beta}{z_3}k_2, s_4 = -\frac{\beta}{z_4}\delta_p, \quad s_5 = -\frac{\beta}{z_5}\delta_b, s_6 = -\frac{\beta}{z_6}k_3, s_7 = -\frac{\beta}{z_7}\delta_b, \tag{56}$$

where z_i and k_i are defined previously. It is obvious to see that the roots s_i are negative since $0 < \beta < 1$. Thus, the equilibrium points of model (7) are asymptotically stable.

Theorem 5 epidemiologically implies that the disease can be eliminated if sustained interventions keep the effective reproduction number below 1 ($R_c < 1$).

5.1.2. Global stability of onchocerciasis-free equilibrium.

The model (7) contains onchocerciasis-Free equilibrium (OFE) E^0, which is globally asymptotically stable (GAS) when $\mathcal{R}_c \leq 1$.
the GAS of model (7), we use the Lyapunov function [65–67]. We define a candidate Lyapunov function for some non-negative constant values L_1, L_2, L_3, and L_4, as follows

$$F(E_p, I_p, E_b, I_b) = L_1 E_p + L_2 I_p + L_3 E_b + L_4 I_b. \tag{57}$$

The time derivative of F in the Caputo-Fabrizio sense is as follows:

$${}^{CF}D_t^{\beta} F = L_1 {}^{CF}D_t^{\beta_2} E_p + L_2 {}^{CF}D_t^{\beta_3} I_p + L_3 {}^{CF}D_t^{\beta_6} E_b + L_4 {}^{CF}D_t^{\beta_7} I_b. \tag{58}$$

Substitute the derivative defined in Equation (7), gives

$$\begin{aligned} {}^{CF}D_t^{\beta} F = {} & L_1\left(\frac{\xi_p(1-\varepsilon)pI_b}{T_b}S_p - (\tau + \sigma_p + \delta_p)E_p\right) \\ & + L_2\left(\sigma_p E_p - (\gamma + \delta_p)I_p\right) \\ & + L_3\left(\frac{\xi_b q I_p}{T_p}S_b - (\sigma_b + \delta_b)E_b\right) + L_4\left(\sigma_b E_b - \delta_b I_b\right). \end{aligned} \tag{59}$$

Rearranging (59) by collecting like terms, gives:

$$\begin{aligned} {}^{CF}D_t^{\beta} F = {} & \left(L_1\frac{\xi_p(1-\varepsilon)p}{T_b}S_p - L_3(\sigma_b + \delta_b)\right)E_b \\ & + \left(L_3\frac{\delta_b q}{T_p}S_b - L_4\delta_b\right)I_b \\ & + \left(L_1\frac{\delta_p(1-\varepsilon)p}{T_b}S_p - L_2(\gamma + \delta_p)\right)I_p \\ & + \left(L_2\sigma_p - L_1(\tau + \sigma_p + \delta_p)\right)E_p. \end{aligned} \tag{60}$$

Assigning values (expression) to the constants that ensures ${}^{CF}D_t^{\beta} F \leq 0$, we have the following:

$$\begin{aligned} & L_1 = (\gamma + \delta_p)\delta_b, L_2 = \xi_b q \delta_b, \\ & L_3 = \sigma_p L_4, L_4 = \xi_p(1-\varepsilon)p(\gamma + \delta_p). \end{aligned} \tag{61}$$

Using the relation in (61), we have the following relations:

$$\begin{aligned} {}^{CF}D_t^{\beta} F = {} & [\xi_b q \delta_b \sigma_p - (\gamma + \delta_p)\delta_b(\tau + \sigma_p + \delta_p)]E_p \\ & + [-\xi_b q \delta_b(\gamma + \delta_p) \\ & + \xi_p \sigma_b(1-\varepsilon)p(\gamma + \delta_p)\frac{\xi_b q}{T_p}S_b]I_p \\ & + [-\xi_p(1-\varepsilon)p\sigma_b(\gamma + \delta_p)(\sigma_b + \delta_b) \\ & + \xi_p(1-\varepsilon)p(\gamma + \delta_p)\sigma_b]E_b \\ & + [(\gamma + \delta_p)\delta_b\frac{\xi_p(1-\varepsilon)p}{T_b}S_p \\ & - \xi_p(1-\varepsilon)p(\gamma + \delta_p)\delta_b]I_b. \end{aligned} \tag{62}$$

We note the term $\frac{\xi_b q}{T_p}S_b$ and $\frac{\xi_p(1-\varepsilon)p}{T_b}S_p$ in the relation in I_p and I_p, respectively. Since $S_b \leq T_b$ and $S_p \leq T_p$, we can upper bound each term as follows:

$$\begin{aligned} {}^{CF}D_t^{\beta} F \leq {} & [\xi_b q \delta_b \sigma_p - (\gamma + \delta_p)\delta_b(\tau + \sigma_p + \delta_p)]E_p \\ & + [-\xi_b q \delta_b(\gamma + \delta_p) \\ & + \xi_p \sigma_b(1-\varepsilon)p(\gamma + \delta_p)\xi_b q\frac{T_b}{T_p}]I_p \\ & + [-\delta_p(1-\varepsilon)p\sigma_b(\gamma + \delta_p)(\sigma_b + \delta_b) \\ & + \delta_p(1-\varepsilon)p(\gamma + \delta_p)\sigma_b]E_b \\ & + [(\gamma + \delta_p)\delta_b\delta_p(1-\varepsilon)p\frac{T_p}{T_b}S_p \\ & - \xi_p(1-\varepsilon)p(\gamma + \delta_p)\delta_b]I_b. \end{aligned} \tag{63}$$

Simplifying further, we have:

$${}^{CF}D_t^{\beta} F \leq Z(R_c - 1)[E_p + E_p + E_b + I_b], \tag{64}$$

where $Z = [(\tau + \sigma_p + \delta_p)(\gamma + \delta_p)(\sigma_b + \delta_b)\delta_b]$. Applying LaSalle's invariance principle, when $R_c \leq 1$ we have ${}^{CF}D_t^{\beta} F \leq 0$,

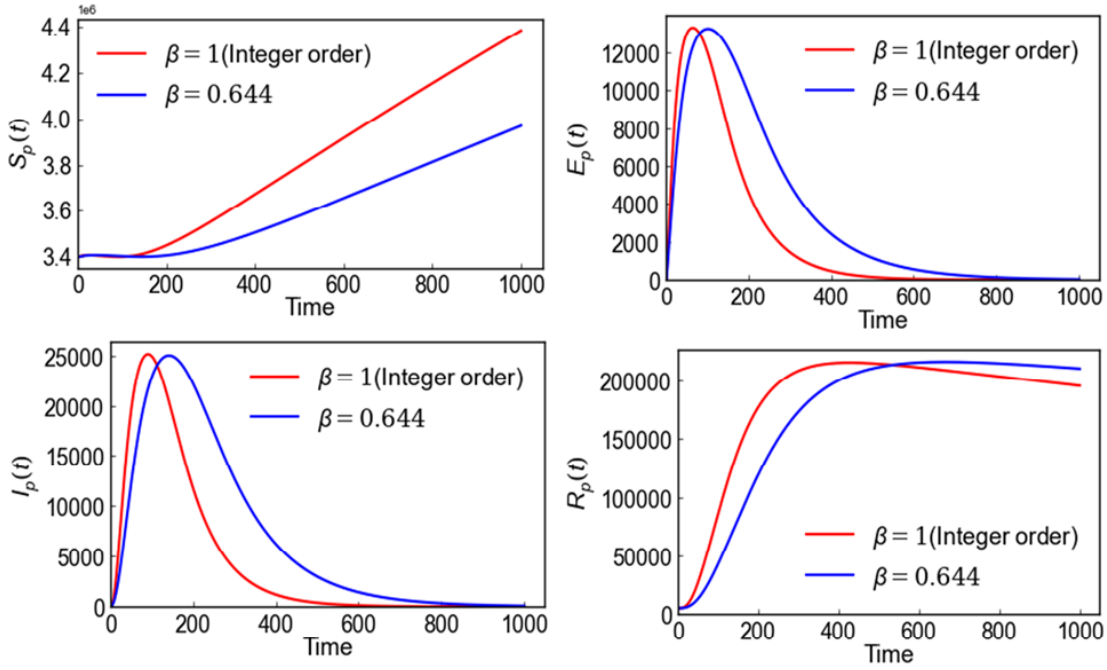

Figure 4. Comparative simulation dynamics of integer-order ($\beta = 1$) and fractional-order ($\beta = 0.644$) models in human populations, model (7).

Table 2. Estimated and fitted parameter values for the model.

Parameters	Range	Value\month	Source
Λ_p	-	45176	assumed
Λ_b	500 - 1000	600	[18, 19]
δ_p	0.0 - 0.0017	0.001299	[20]
δ_b	0.00118 - 0.0714	0.068321	[74–76]
ξ_p	0.0 -1.0	0.8354	[19, 77]
ξ_b	0.0 - 1.0	0.7258	[75, 77]
σ_p	0.00137 - 0.0363	0.00139	[74–76]
σ_b	0.00714 - 0.01667	0.095	[74, 75]
τ	-	0.566	assumed
γ	-	0.2584	fitted
q	-	0.0855	[19, 77]
p	-	0.0982	[19]
ϵ	-	0.513	assumed

meaning F is non-increasing. The largest invariant set where ${}^{CF}D_t^{\beta}F \leq 0$, is the $E_p = I_p = E_b = I_b = 0$ which correspond to DFE, E^0. Thus, the system is GAS by LaSalle's invariance principle and converges to E^0 when $R_c \leq 1$. The Lyapunov function ensures that the trajectory tends to E^0, meaning the disease will be eradicated if $R_c \leq 1$.

5.2. Onchocerciasis Endemic Equilibrium Points (OEEP)

At this equilibrium, onchocerciasis continues to exist within a population. Equation (65) is the endemic equilibrium points of the state variables in terms of ψ_p^* and ψ_b^*.

$$S_p = \frac{\Lambda_p}{\psi_p^* + \delta_p}, E_p = \frac{\Lambda_p \psi_p^*}{k_1(\psi_p^* + \delta_p)}, I_p = \frac{\Lambda_p \sigma_p \psi_p^*}{k_1 k_2(\psi_p^* + \delta_p)},$$
$$R_p = \frac{\Lambda_p \psi_p^*(\tau k_2 + \sigma_p \gamma)}{\delta_p k_1 k_2(\delta_p^* + \delta_p)}, \tag{65}$$
$$S_b = \frac{\Lambda_b}{\psi_b^* + \delta_b}, E_b = \frac{\Lambda_b \psi_b^*}{k_3(\psi_b^* + \delta_b)}, I_b = \frac{\Lambda_b \sigma_b \delta_b^*}{\delta_b k_3(\psi_b^* + \delta_b)}.$$

$$T_p(t) = S_p(t) + E_p(t) + I_p(t) + R_p(t),$$
$$T_b(t) = S_p(t) + E_p(t) + I_p(t). \tag{66}$$

Substituting all the value of state variables of (65) into (66), we have:

$$T_P = \frac{k_1 k_2 \Lambda_P + k_2 \Lambda_P \psi_p^* + k_2 \Lambda_p \sigma_p \lambda_p^*}{k_1 k_2(\lambda_p^* + \delta_p)},$$
$$T_b = \frac{k_3 \Lambda_p + \delta_p \Lambda_b \psi_b^* + \Lambda_b \sigma_b \psi_b^*}{\delta_b k_3(\psi_b^* + \delta_b)}. \tag{67}$$

Substituting all the values of concerned state variables of (65) into (4), we have;

$$(\delta_b k_3 \Lambda_p + (\delta_b \Lambda_b + \delta_b \sigma_p \Lambda_p)\psi_p^*)\psi_p^* - \xi_p(1-\epsilon)p\Lambda_b \sigma_b \psi_b^* \psi_p^* = 0. \tag{68}$$

Similarly, substituting all the values of the concerned state variables of (65) into (5) yields:

$$\psi_b^* = \frac{\xi_b q \Lambda_p \sigma_p \psi_p^*}{k_1 k_2 \Lambda_p + (k_2 \Lambda_p + \sigma_p \Lambda_p)\psi_p^*}. \tag{69}$$

Substituting (69) into (68) and simplify.

$$\psi_p^*(A\psi_p^* + C) = 0, \tag{70}$$

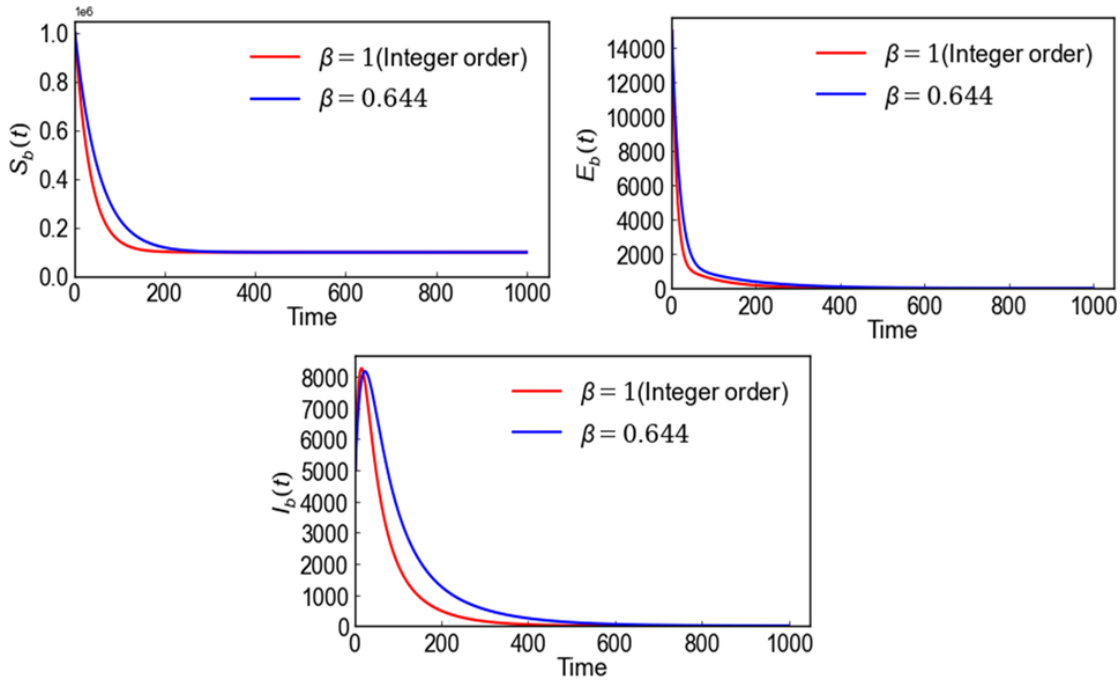

Figure 5. Comparative simulation dynamics of integer-order ($\beta = 1$) and fractional-order ($\beta = 0.644$) models in vector populations, model (7).

where;

$$A = \delta_b k_3 \Lambda_b + (k_2 \Lambda_p + \sigma_b \Lambda_p) + (\Lambda_b \delta_b + \Lambda_b \sigma_p)\xi_b q \Lambda_p \sigma_p,$$
$$C = \delta_b k_1 k_2 k_3 \Lambda_b \Lambda_p \left[1 - \left(\sqrt{\frac{\xi_p \xi_b (1-\epsilon) p q \sigma_b \sigma_p}{k_1 k_2 k_3 \delta_b}}\right)^2\right]. \tag{71}$$

From (70), we have, either

$$\psi_p^* = 0 \quad \text{or} \quad A\psi_p^* + C = 0. \tag{72}$$

Hence, we claim that model (7) has a unique endemic equilibrium point if $\mathcal{R}_c > 1$.

5.2.1. Global stability of endemic equilibrium point

Let

$$\mathcal{D}^* = \{\left(S_p^*, E_p^*, I_p^*, R_p^*, S_b^*, E_b^*, I_b^*\right) \in \mathcal{D}^*\} \tag{73}$$

be a stable manifold of $\mathcal{D}^*$. The endemic equilibrium point (EEP) of model (1) is globally asymptotically stable (GAS) in $\mathcal{D}^*$ with the conditions that $\tau = 0$ whenever $\mathcal{R}_c > 1$. Let $\mathcal{V}$ be a Goh-Volterra type of Lyapunov function given below.

$$\begin{aligned}\mathcal{V} = &\left(S_p - S_p^* - S_p^* ln\frac{S_p}{S_p^*}\right)\\ &+ \left(E_p - E_p^* - E_p^* ln\frac{E_p}{E_p^*}\right) + \frac{k_1}{\sigma_p}\left(I_p - I_p^* - I_p^* ln\frac{I_p}{I_p^*}\right)\\ &+ \frac{k_1 k_2}{\sigma_p \gamma}\left(R_p - R_p^* - R_p^* ln\frac{R_p}{R_p^*}\right)\\ &+ \left(S_b - S_b^* - S_b^* ln\frac{S_b}{S_b^*}\right) + \left(E_b - E_b^* - E_b^* ln\frac{E_b}{E_b^*}\right)\\ &+ \frac{k_3}{\sigma_b}\left(I_b - I_b^* - I_b^* ln\frac{I_b}{I_b^*}\right).\end{aligned} \tag{74}$$

Differentiating (74) with respect to time give:

$$\begin{aligned}{}^{CF}D_t^\beta V = &\left(1 - \frac{S_p^*}{S_p}\right){}^{CF}D_t^\beta S_p + \left(1 - \frac{E_p^*}{E_p}\right){}^{CF}D_t^\beta E_p\\ &+ \frac{k_1}{\sigma_p}\left(1 - \frac{I_p^*}{I_p}\right){}^{CF}D_t^\beta I_p\\ &+ \frac{k_1 k_2}{\sigma_p \gamma}\left(1 - \frac{R_p^*}{R_p}\right){}^{CF}D_t^\beta R_p + \left(1 - \frac{S_b^*}{S_b}\right){}^{CF}D_t^\beta S_b\\ &+ \left(1 - \frac{E_b^*}{E_b}\right){}^{CF}D_t^\beta E_b + \frac{k_3}{\sigma_b}\left(1 - \frac{I_v^*}{I_b}\right){}^{CF}D_t^\beta I_b.\end{aligned} \tag{75}$$

Substituting (7) with $\tau = 0$ into (75), we have:

$$\begin{aligned}{}^{CF}D_t^\beta V = &\left(1 - \frac{S_p^*}{S_p}\right)\left(\Lambda_p - \psi_p S_p - \delta_p S_p\right)\\ &+ \left(1 - \frac{E_p^*}{E_p}\right)\left(\psi_p S_h - k_1 E_p\right)\\ &+ \frac{k_1}{\sigma_h}\left(1 - \frac{I_p^*}{I_p}\right)\left(\sigma_p E_p - k_2 I_p\right)\\ &+ \frac{k_1 k_2}{\sigma_p \gamma}\left(1 - \frac{R_p^*}{R_p}\right)\left(\gamma I_p - \delta_p R_p\right)\\ &+ \left(1 - \frac{S_b^*}{S_b}\right)(\Lambda_b - \psi_b S_b - \delta_b S_b)\\ &+ \left(1 - \frac{E_b^*}{E_b}\right)(\psi_b S_b - k_3 E_b)\\ &+ \frac{k_3}{\sigma_b}\left(1 - \frac{I_b^*}{I_b}\right)(\sigma_b E_b - \delta_b I_b).\end{aligned} \tag{76}$$

Consider relations:

$$\begin{aligned}\Lambda_p = \psi_p S_p^* + \delta_p S_p^*, k_1 E_p^* &= \psi_p S_p^*, k_2 I_p^* = \sigma_p E_p^*,\\ k_3 E_b^* = \psi_b S_b^*, \delta_p R_p^* &= \gamma I_p^*, \delta_b I_b^* = \sigma_b E_b^*.\end{aligned} \tag{77}$$

Substituting the relations in (77) into (76) and simplify yield:

$$\begin{aligned} {}^{CF}D_t^{\beta}V \leq\ & \delta_p S_p^*\left(2-\frac{S_p}{S_p^*}-\frac{S_p^*}{S_p}\right) \\ & +\psi_p S_p^*\left(5-\frac{S_p^*}{S_p}-\frac{S_pE_p^*}{S_p^*E_p}-\frac{E_pI_p^*}{E_p^*I_p}-\frac{R_p}{R_p^*}-\frac{I_pR_p^*}{I_p^*R_p}\right) \\ & +\delta_b S_b^*\left(2-\frac{S_b}{S_b^*}-\frac{S_b^*}{S_b}\right) \\ & +\psi_b S_b^*\left(4-\frac{S_b^*}{S_b}-\frac{S_bE_b^*}{S_b^*E_b}-\frac{I_b}{I_b^*}-\frac{E_bI_b^*}{E_b^*I_b}\right). \end{aligned} \tag{78}$$

Using the relation of arithmetic mean to geometric mean, we then have;

$$\begin{aligned} & \left(2-\frac{S_p}{S_p^*}-\frac{S_p^*}{S_p}\right)\leq 0, \\ & \left(5-\frac{S_p^*}{S_p}-\frac{S_pE_p^*}{S_p^*E_p}-\frac{E_pI_p^*}{E_p^*I_p}-\frac{R_p}{R_p^*}-\frac{I_pR_p^*}{I_p^*R_p}\right)\leq 0, \\ & \left(2-\frac{S_b}{S_b^*}-\frac{S_b^*}{S_b}\right)\leq 0, \left(4-\frac{S_b^*}{S_b}-\frac{S_bE_b^*}{S_b^*E_b}-\frac{I_b}{I_b^*}-\frac{E_bI_b^*}{E_b^*I_b}\right)\leq 0. \end{aligned} \tag{79}$$

Hence, we have ${}^{CF}D_t^{\beta}V \leq 0$ with conditions that $\tau = 0$ and $\mathcal{R}_c > 1$, since all the concerned variable in the model such as $S_p, E_p, I_p, R_p, S_b, E_b$, and I_b are at steady state (endemic steady state), substitute into the concerned variable of (1) to give:

$$\begin{aligned} \lim_{t\to\infty}\left(S_p(t), E_p(t), I_p(t), R_p(t), S_b(t), E_b(t), I_b(t)\right) \\ \to \left(S_p, E_p, I_p, R_p, S_b, E_b, I_b\right). \end{aligned} \tag{80}$$

Hence, by Lassalle's invariant principle [68], the globally asymptotically stable (GAS) is established. The theorem implies that, regardless of the initial infectiousness in the society, onchocerciasis can escalate if the number of secondary cases produced by a single infected person is greater than one and if those individuals are not receiving treatment.

6. 3-Step Adam-Bashforth predictor scheme and numerical simulations

We apply the idea of the three-step fractional Adams-Bashforth numerical scheme derived in Ref. [49] for the numerical solutions of our fractional onchocerciasis model (7) - (8). Hence, utilizing the definition of Caputo-Fabrizio fractional derivative as presented in Equation (1) and its associate integral operator Equation (3), the incremental change in the numerical solution from t_n to $t_{(n+1)}$, gives:

$$\begin{aligned} u(t_{n+1})-u(t_n) = \frac{(1-\beta)}{M(\beta)}[\varphi(t_n,u(t_n))-\varphi(t_{n-1},u(t_{n-1}))]+ \\ \frac{\beta}{M(\beta)}\int_{t_n}^{t_{n+1}}\varphi(t,u(t))\,dt. \end{aligned} \tag{81}$$

The integral in Equation (81) is approximated using a Lagrange polynomial defined by Equation (82).

$$P_2(t) = \sum_{i=0}^{2}\varphi(t_{n-i},u_{n-i})L_i(t), \tag{82}$$

where:

$$\begin{aligned} L_0(t) &= \frac{(t-t_{n-1})(t-t_{n-2})}{(t_n-t_{n-1})(t_n-t_{n-2})}, \\ L_1(t) &= \frac{(t-t_n)(t-t_{n-2})}{(t_{n-1}-t_n)(t_{n-1}-t_{n-2})}, \\ L_2(t) &= \frac{(t-t_n)(t-t_{n-1})}{(t_{n-2}-t_n)(t_{n-2}-t_{n-1})}. \end{aligned} \tag{83}$$

Thus, the numerical scheme is

$$\begin{aligned} u(t_{n+1}) = u(t_n) + \frac{1}{M(\beta)}\left[(1-\beta)+\frac{23\beta h}{12}\right]\varphi(t_n,u_n) \\ -\frac{1}{M(\beta)}\left[(1-\beta)+\frac{16\beta h}{12}\right]\varphi(t_{n-1},u_{n-1})+\frac{1}{M(\beta)}\frac{5\beta h}{12}\varphi(t_{n-2},u_{n-2}). \end{aligned} \tag{84}$$

We estimate the truncation error $E_k(t)$ for the three-step Adams Bashforth scheme using the idea of error estimate for Lagrange interpolation polynomial in Ref. [69] defined by;

$$E_k(t) = \frac{\varphi^{(k+1)}(\xi_n,u(\xi_n))}{(k+1)!}\prod_{i=0}^{k}(t-t_{n-i}).$$

Subsequently, for ease of computation, we shall consider the normalized constant $M(\beta) = 1$.

6.1. Parameter estimation

We use the onchocerciasis reported infectious cases based on monthly collected data provided by Ghana Health Services from January 2008 to December 2015, publicly available in Ref. [18, 20, 70]. The human infectious compartment was fitted to the reported infected cases. Ghana's population at risk of contracting onchocerciasis is estimated to be $3,400,000$ as of the time data were gathered [20], while the following initial conditions were used for curve fitting: $S_p = 3,400,0000, E_p = 5000, I_p = 150, R_p = 1400, S_b = 140000, E_b = 7000, I_b = 5000$ [20, 70]. A Python code was developed utilizing a "built-in SciPy" algorithm available in Python version 3.12.1 for parameter estimation. We use the non-linear least squares (NLS) method to estimate the model's parameter values. Table 2 presents the estimated parameters and some published parameters. Figure 2(a) illustrates fitting result. The fitting's fractional order differentiation parameter β was estimated as $\beta = 0.644$. The statistical metrics, coefficient of determination (R^2), and mean absolute percentage error (MAPE) were utilized for model fit evaluation. We obtained $R^2 = 0.9950$ and MAPE = 7.68%, which indicate good agreement between observed and predicted data [71–73]. Hence, it shows that incorporating memory effects in modeling onchocerciasis dynamics improves the fit accuracy. Figure 2(b) presents box plots that illustrate the agreement in variability and central tendency. This further confirm that the fitting results effectively captures the observed dynamics.

6.2. Sensitivity analysis

Sensitivity analysis assesses how each parameter impacts the infectious disease dynamics under investigation [39]. To investigate the most influential parameter in model (7), local

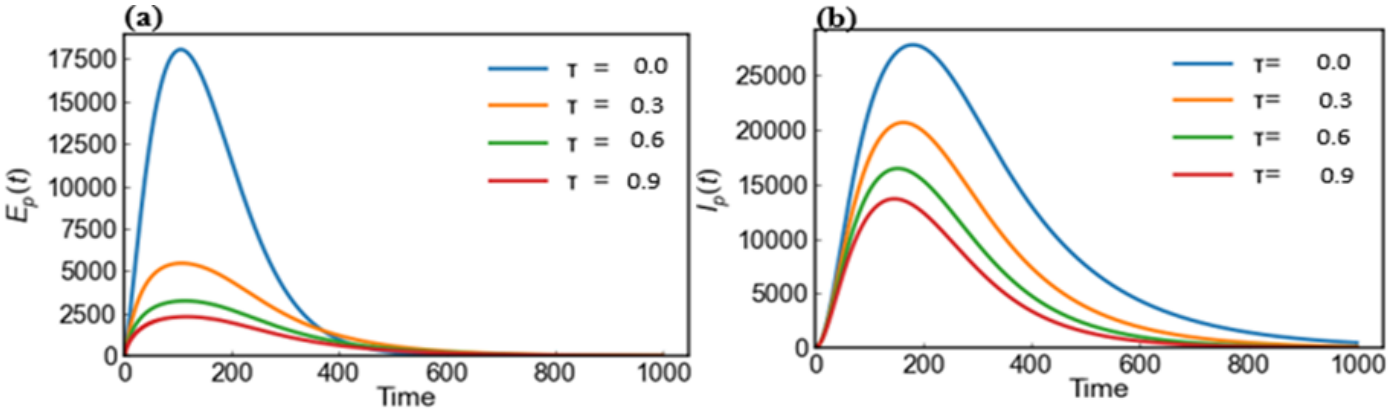

Figure 6. Effect of varying early treatment rate (τ) on (a) Exposed human and (b) infectious human populations.

sensitivity analysis of each parameter is performed, in light Ref.[78]. The normalized local sensitivity index, $\chi_{\theta}^{\mathcal{R}_c}$, is introduced to accomplish this. The normalized forward sensitivity index of the effective reproduction number $\mathcal{R}_c$, to a parameter θ denoted by $\chi_{\theta}^{\mathcal{R}_c}$ is defined as the ratio of the realative change in $\mathcal{R}_c$ to the relative change in θ, is expressed as:

$$\chi_{\theta}^{\mathcal{R}_c} = \frac{\partial \mathcal{R}_c}{\partial \theta} \cdot \frac{\theta}{\mathcal{R}_c}.$$

The Figure 3 displays the sensitivity index parameters from the model equation related to the effective reproduction number. It shows that the vector management control and early treatment rates are the most influential factors in decreasing the effective reproduction number. In contrast, the effective contact rates of humans and vectors significantly increase the effective reproduction number.

6.3. Numerical simulations

Table 2 parameters value and the initial condition are used to numerically solve the model (7) via the three-step Adams-Bashforth method with code written in Python 3.12.1.

Figures 4 and 5 illustrate the dynamics of human and vector populations, respectively. The figures show how the number of infected human individuals peaks before gradually declining. The graphs indicate that the vector population initially carries a high burden of exposed and infectious individuals due to a larger number of exposed and infectious vectors. Over time, the transmission dynamics change, leading to a drastic decrease in the number of new vectors that become exposed or infectious. However, the fractional-order dynamics plots offer a more realistic depiction of non-instantaneous transitions in onchocerciasis progression. Considering fractional-order plots, we investigate the impact of the early treatment rate (τ) on the exposed and infectious humans and the vector management control rate (ϵ) on both the exposed and infectious humans and vectors.

Equation (85) calculates the approximate percentage reduction in infection peak prevalence due to increased intervention strategy intensity.

$$\text{Percentage Reduction} \approx \left(1 - \frac{P(\kappa = \kappa_i^*)}{P(\kappa = 0)}\right) \times 100\%. \tag{85}$$

where $\kappa = (\tau, \epsilon)$ are the intervention strategies, $\kappa_i^*(\kappa_i^* = 0.3, 0.6, 0.9)$ is the intensity and $P(\kappa = \kappa_i^*)$ is the peak value obtained for applying the intervention κ_i^*, and $P(\kappa = 0)$ is the peak value no intervention is apply.

Figure 6 illustrates the impact of early treatment rates on exposed and infectious human populations. Without treatment ($\tau = 0.0$), the exposed population peaks at approximately $17,500$. As the early treatment rate coverage increases to $\tau = 0.3(30\%), 0.6(60\%)$, and $0.9(90\%)$, the peak prevalence decreases to about $7,000, 3,000$, and $1,500$, indicating reductions of about 60%,82.8%, and 90%, respectively. Similarly, the infectious population peaks at approximately $25,000$ with no treatment. With early treatment rate τ coverage of $0.3(30\%), 0.6(60\%)$, and $0.9(90\%)$, the peak declines to $17,000, 10,000$, and $6,000$, reflecting reductions of about $32\%, 60\%$, and 76%. This decrease in exposed (E_p) and infectious (I_p) populations at different treatment levels informs policymakers of the potential benefits of reduced disease burden associated with each level of early treatment effort.

In particular, the exposed population (E_p) experiences a relatively higher reduction in prevalence with increasing treatment rates compared to the infectious population (I_p). For example, at $\tau = 0.9$, there is an approximate 90% reduction in E_p and a 76% reduction in I_p. This finding indicates that policymakers should: (a) prioritize treatments that target individuals immediately after exposure, as this strategy may prove more cost-effective than attempting to manage already infectious cases; and (b) strive to reduce the E_p population by at least 90% to mitigate infections and ultimately eliminate transmission. However, in practical settings, onchocerciasis primarily affects impoverished countries, particularly in villages where health facilities for early screening, diagnosis, and timely treatment are often lacking. Implementation of this may suffer setbacks if not adequately planned.

Figure 7 shows how varying the vector management control rate (ϵ) affects the onchocerciasis infection peak prevalence. As ϵ increases, there is a marked reduction in exposed and infectious individuals in both human and vector populations. With no vector control measures ($\epsilon = 0$), the disease spreads rapidly, reaching high peak levels for both hu-

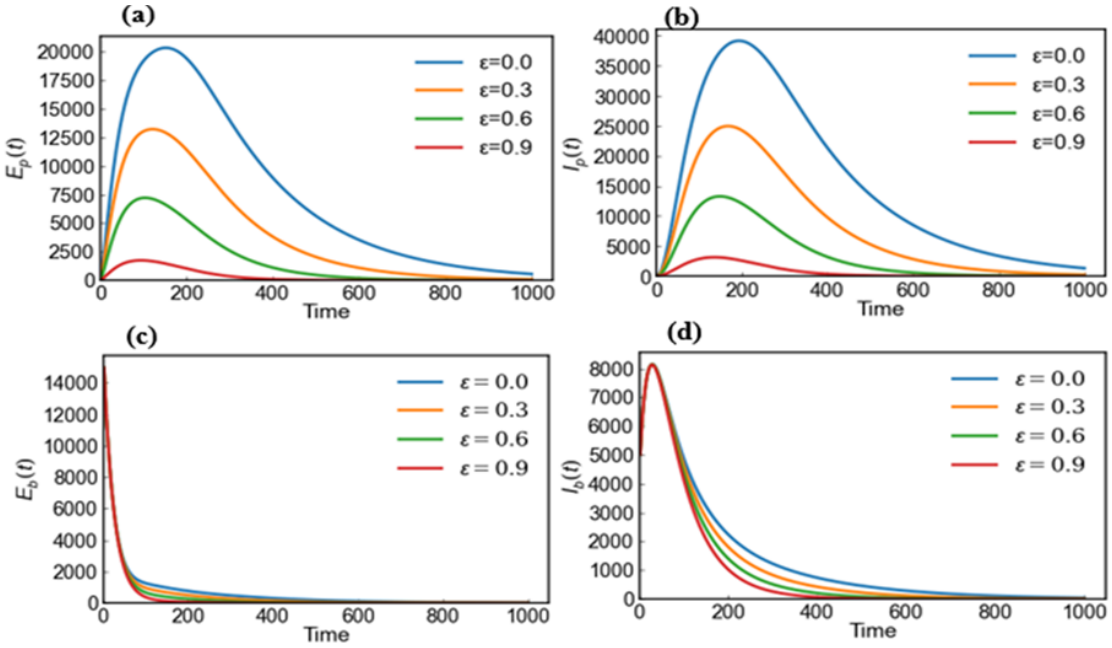

Figure 7. Effect of varying vector control rate (τ) on (a) Exposed human, (b) Infectious human populations, and (c) Exposed vector (d) Infectious vector populations.

man and vector infections (Figures 7(a)-(b)). As ϵ increases to 0.3, 0.6, 0.9, the human exposed population decreases by approximately 35%, 62.5%, 90%, respectively, while the infectious human population reduces by about 32%, 59%, and 89% (Figures 7(a)-(b)). These reductions stem from significant, albeit smaller, decreases in vector populations (Figures 7(c)-(d)). This reinforces the critical role of vector management control interventions in lessening the impact of onchocerciasis disease and safeguarding public health.

These findings entail that policymakers can establish goals, such as achieving an 80% reduction in peak infections, and allocate resources to increase τ sufficiently to meet that target. Supplemented by a high ϵ rate of at least 60%, this can tremendously mitigate the spread of onchocerciasis in a population by up to 90%.

Figure 8 illustrates surface plots showing the combined impact of control parameters: early treatment rate (τ), vector control rate (ϵ), and infectious treatment rate (γ) on the effective basic reproduction number R_c, with the pink translucent plane indicating the policy threshold ($R_c = 1$). At high values of both $\tau \gtrsim 0.4$ and $\gamma \gtrsim 0.6$, the surface is pushed below the threshold, $R_c < 1$, indicating disease elimination, while the risk region is at $\tau \lesssim 0.2$ and $\gamma \lesssim 0.3$, leading to $R_c > 1$, which indicates disease persistence, highlighting that intensified interventions are required. The risk region in Figure 8(b) is at $\tau \lesssim 0.3$ and $\epsilon \lesssim 0.3$, while disease elimination is set at $\tau \gtrsim 0.4$ and $\epsilon \gtrsim 0.5$. We note that when $\tau = \epsilon = 0$, the analysis of the basic reproduction number R_0 shows that with an increase in ξ_p and ξ_b or p and q, R_0 also increases.

7. Impact of memory effects on onchocerciasis dynamics

Understanding the memory effects helps in designing effective intervention strategies. Analysis of integer-order ($\beta = 1.0$) and fractional-order ($\beta < 1$) models reveals that fractional dynamics significantly alter disease trajectories by introducing memory effects that slow the progression of infections and prolong disease persistence in the populations. This reflects real-world scenarios where disease progression and recovery are influenced by past states, making fractional models more realistic for onchocerciasis dynamics. While integer-order models depict rapid epidemic peaks and swift declines, fractional-order models result in similar but wider peaks and longer infectious periods, as demonstrated by the delayed and broadened peaks observed in exposed and infectious populations (Figures 4 and 5). Thus, using integer models for onchocerciasis control risks underestimating the resilience of the disease due to memory effects. This could lead to premature relaxation of interventions and ultimately, failure to eliminate the disease. Fractional-order models avoid this pitfall by accounting for memory effects that prolong infection dynamics, ensuring that policy and resource planning match the realistic persistence of onchocerciasis in endemic regions.

Analysis of the integer and fractional models across varying fractional orders highlights the extended and heterogeneous spread inherent in onchocerciasis, which the classical models overlook. These will better inform policymakers to enhance intervention strategies to reduce and potentially eliminate onchocerciasis. Figures 9 and 10 show time series plots of the fractional model with distinct fractional orders ($\beta = 0.644, 0.544$, and $\beta = 0.444$) alongside the integer model counterpart. The values $beta = 0.544$ and $\beta = 0.444$ are chosen arbitrarily, less than the fit fractional order ($beta = 0.644$). Fig-

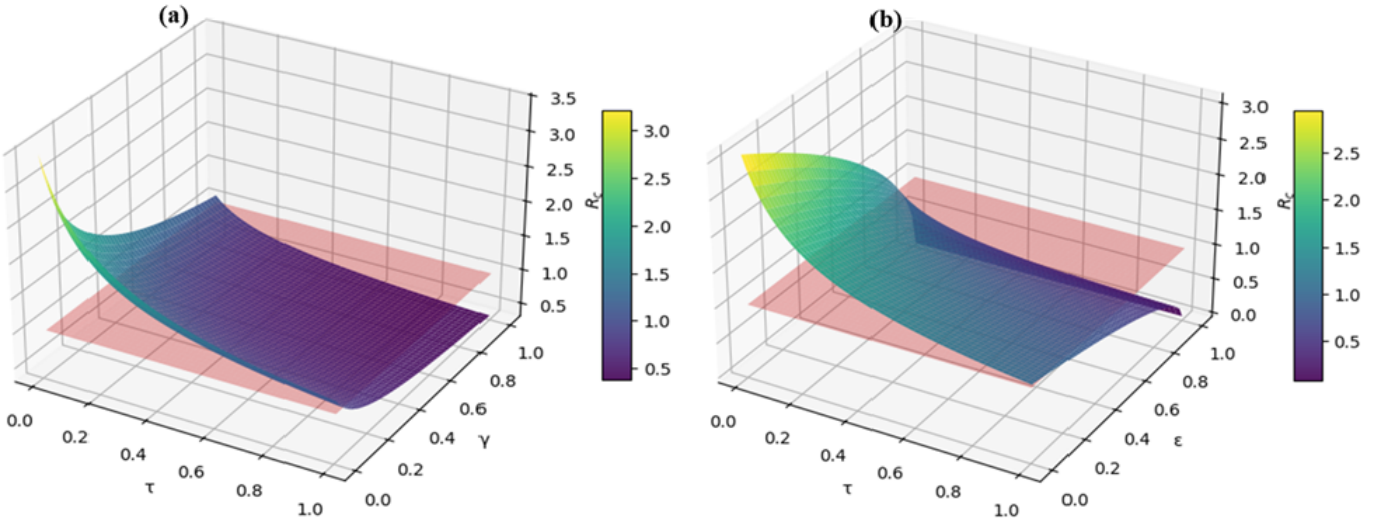

Figure 8. 3D Surface Plots Illustrating the Effects of (a) Early Treatment Rate (τ) and Infectious Treatment Rate (γ), and (b) Early Treatment Rate (τ) and Vector Control Rate (ϵ), on the Effective Reproduction Number ($\mathcal{R}_c$). The pink threshold plane at $\mathcal{R}_c = 1$ marks the critical boundary for disease control.

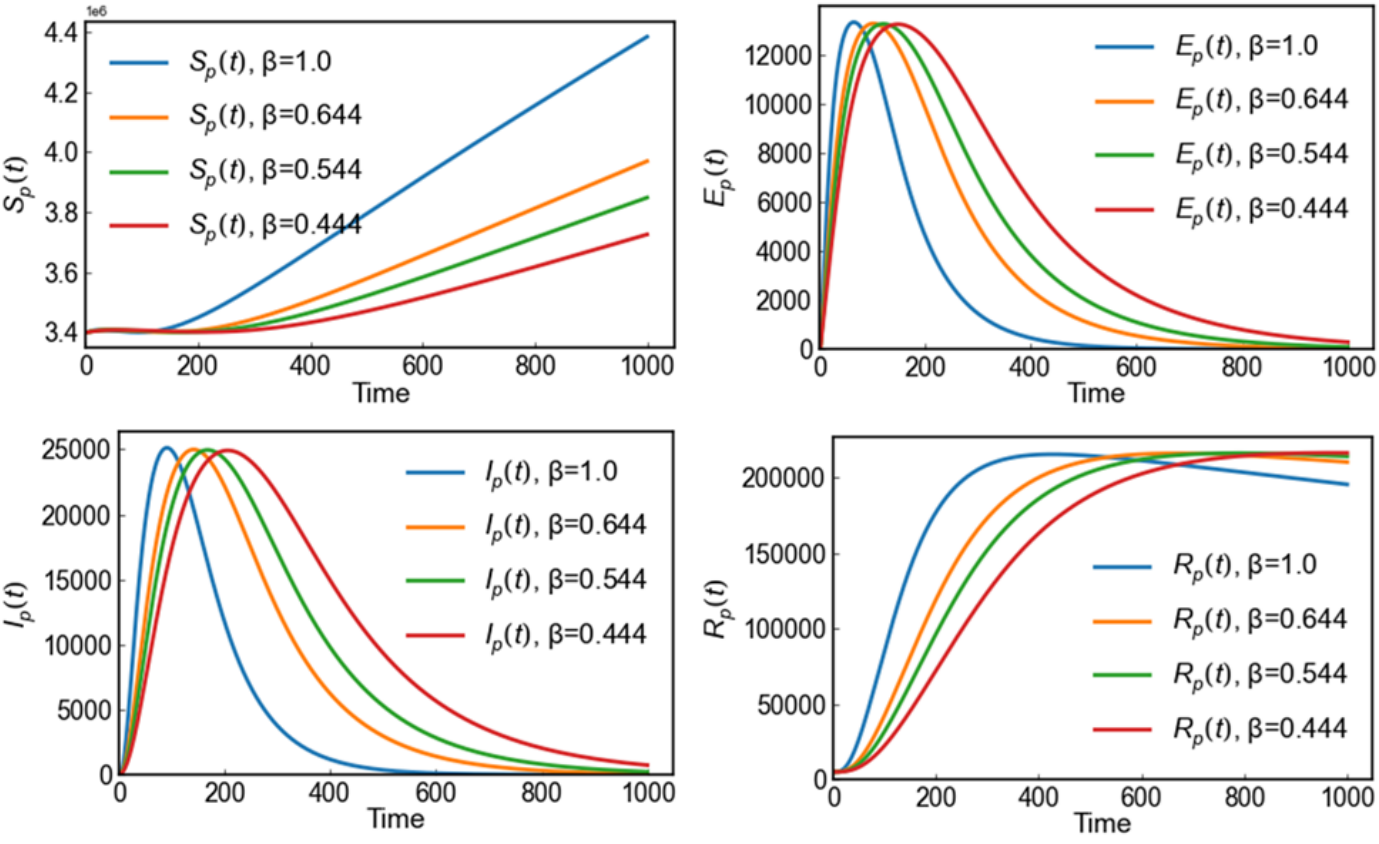

Figure 9. Time series comparative analysis of integer ($\beta = 1.0$) and fractional order ($\beta = 0.644, 0.544, 0.444$) models in human dynamics, model (7).

ures 9 reveal that when β is high, individuals in E_p transition to I_p quickly, leading to a rapid rise in active cases, suggesting that early containment measures such as treatment and vector management must be implemented swiftly to prevent a surge in infectious individuals. Conversely, with lower β values, the progression is more gradual, providing a wider window for intervention; however, complacency can lead to persistent infections if interventions are not consistently applied. Figures 10 show that E_b and I_b populations decline more rapidly at higher β values, while at lower β, the population decline is gradual.

These findings indicate that the fractional-order modeling offers a more realistic view of onchocerciasis dynamics over time. It emphasizes that elimination efforts necessitate sustained vector control measures, earlier and repeated rounds of

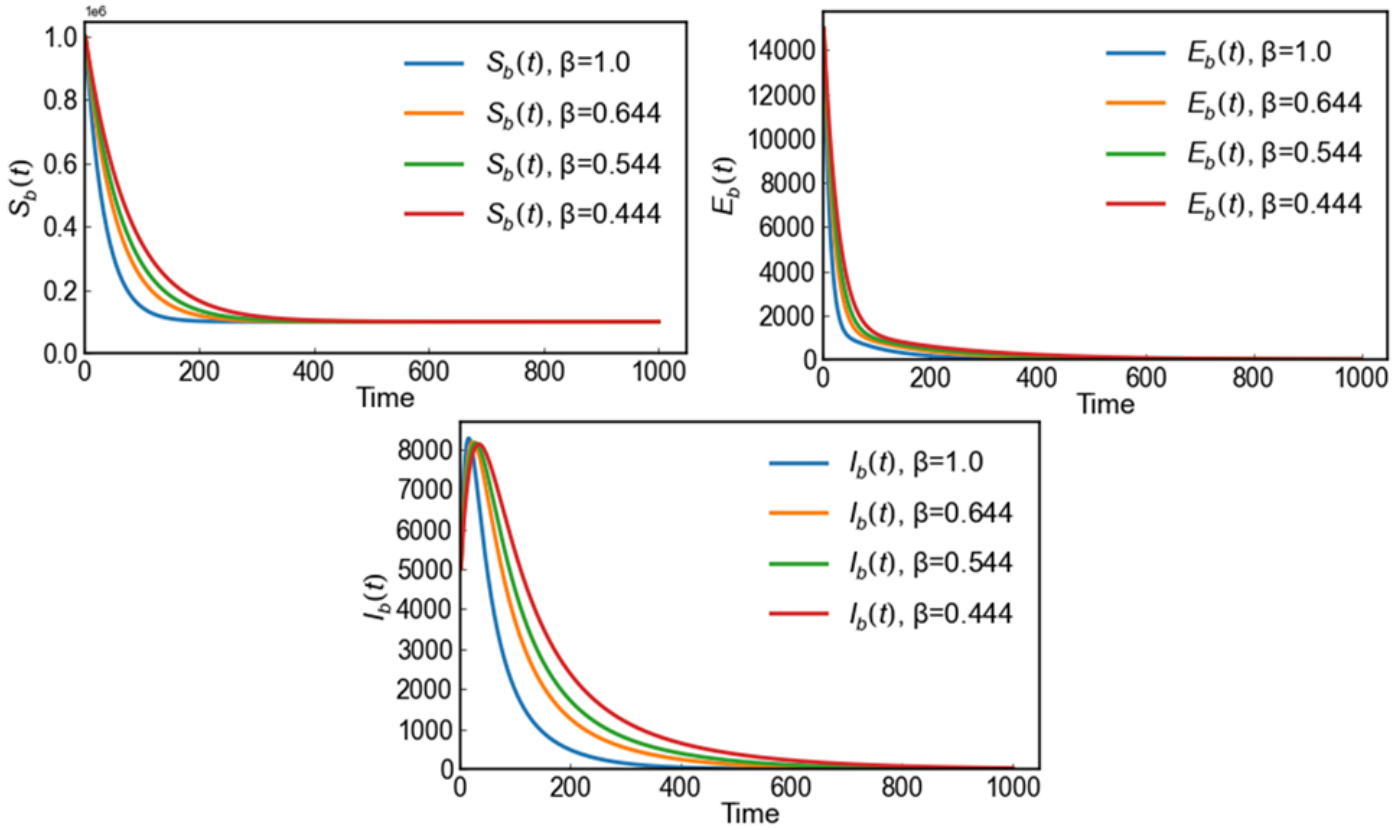

Figure 10. Time series comparative analysis of integer ($\beta = 1.0$) and fractional order ($\beta = 0.644, 0.544, 0.444$) models in vector dynamics, model (7).

MDA with ivermectin, and consistent resource allocation to prevent lingering infections that could reignite transmission. However, in resource-limited settings, policies should prioritize high-endemic regions for MDA, early treatment, and vector control, engage community volunteers to clear vector breeding sites, detect symptoms and report early, and combine control efforts with other NTD (like lymphatic filariasis) programs to save costs and human resources.

8. Conclusion

This study presents a deterministic model examining interactions between humans and vectors within a habitat, dividing disease transmission dynamics into seven compartments. Our model incorporates early treatment and vector management as intervention strategies. Given that the disease dynamics leave an immunological and epidemiological memory in humans, predicting future disease states requires considering both their current and past states. The previous integer-order onchocerciasis model cannot accommodate this. We propose a new compartmentalized model using a fractional derivative in the Caputo-Fabrizio sense for improved intervention control analysis. We establish the existence and uniqueness of the model's solution using the fixed-point theorem and an iterative method. The disease-free equilibrium solution is locally asymptotically stable, while global asymptotic stability for both disease-free and endemic equilibria is demonstrated through a Lyapunov function. Parameters are estimated by fitting the model to confirmed onchocerciasis case data from Ghana Health Services [18, 20]. Data fitting indicates that the model's differential equations have an order of 0.644, with $R^2 = 0.9950$ and MAPE =7.68%, suggesting that fractional-order differential equations provide a good fit. Sensitivity analysis reveals that vector control (ε) and early treatment (τ) are more effective at reducing the effective reproduction number R_c, while an increase in contact rates (ξ_p, ξ_b) between vector and human (ξ_b) elevates it. Numerical solutions of the model using the three-step fractional Adams-Bashforth method suggest that the control measures—early treatment and vector management—effectively eradicate the disease. Comparative numerical simulation of the fractional order ($\beta < 1$) model and integer order ($\beta = 1$) model reveals rapid epidemic peaks and swift declines with the integer model. In contrast, fractional-order models result in similar but wider peaks and longer infectious periods, influenced by the disease memory effect. This shows that control policy using an integer model may underestimate the disease's resilience and could lead to premature relaxation of interventions. In contrast, fractional order models avoid this pitfall and should be used for control policy design.

Findings indicate that fractional-order modeling offers a better view of disease dynamics, and elimination efforts must prevent unnoticed infections through long-term interventions, resource allocation, and vigilant surveillance to reduce the disease's memory index β toward elimination. Thus, we assert

that onchocerciasis can be controlled at least up to 90% with this approach.

Data availability challenges hindered the incorporation of cost-effectiveness analysis into our model. Future research should explore onchocerciasis co-infection modeling with other relevant filarial parasites (such as *Loa loa, Wuchereria bancrofti*, and *Mansonella species*), where shared treatments (like ivermectin) and immunological overlaps are significant. The Atangana-Baleanu derivative is an alternative fractional derivative that can be explored.

Data Availability

All research data are included in the submitted manuscript file.

Acknowledgment

This work was supported by Universiti Sains Malaysia, Bridging Grant with Project No: R501-LR-RND000-0000001593-0000. The authors thank the School of Mathematical Sciences, Universiti Sains Malaysia, for providing facilities used for the study. The scholarship given to Danat Nanle by TETFund Nigeria is duly appreciated.

References

[1] H. C. Turner, M. Walker, M. D. French, I. M. Blake, T. S. Churcher & M. G. Basanez, "Neglected tools for neglected diseases: mathematical models in economic evaluations", Trends in parasitology **30** (2014) 562. https://doi.org/10.1016/j.pt.2014.10.001.

[2] S. Jawahar, N. Tricoche, C. A. Bulman, J. Sakanari & S. Lustigman, "Drugs that target early stages of onchocerca volvulus: A revisited means to facilitate the elimination goals for onchocerciasis", PLoS Neglected Tropical Diseases **15** (2021) 0009064. https://doi.org/10.1371/journal.pntd.0009064.

[3] P. T. Cantey, S. L. Roy, D. Boakye, U. Mwingira, E. A. Ottesen, A. D. Hopkins & Y. K. Sodahlon, "Transitioning from river blindness control to elimination: steps toward stopping treatment", International health **10** (2018) 7. https://doi.org/10.1093/inthealth/ihx049.

[4] R. S. Nicholls, S. Duque, L. A. Olaya, M. C. Lopez, S. B. S ´ anchez, A. L. Morales & G. I. Palma, "Elimination of onchocerciasis from Colombia: first proof of concept of river blindness elimination in the world", Parasites & vectors **11** (2018) 1. https://doi.org/10.1186/s13071-018-2821-9.

[5] M. Sauerbrey, L. J. Rakers & F. O. Richards, "Progress toward elimination of in the Americas", International health **10** (2018) 71. https://doi.org/10.1093/inthealth/ihx039.

[6] D. N. Udall, "Recent updates on onchocerciasis: diagnosis and treatment", Clinical infectious diseases **44** (2007) 53. https://doi.org/10.1086/509325.

[7] L. Frallonardo, F. Di Gennaro, G. G. Panico, R. Novara, E. Pallara, S. Cotugno, G. Guido, E. De Vita, A. Ricciardi, V. Totaro et al., "Onchocerciasis: current knowledge and future goals", Frontiers in Tropical Diseases **3** (2022) 986884. https://doi.org/10.3389/fitd.2022.986884.

[8] R. K. Prichard, M.-G. Basanez, B. A. Boatin, J. S. McCarthy, H. H. Garcia, G. J. Yang, B. Sripa & S. Lustigman, "A research agenda for helminth diseases of humans: intervention for control and elimination", PLoS neglected tropical diseases **6** (2012) 1549. https://doi.org/10.1371/journal.pntd.0001549.

[9] S. Lustigman, R. K. Prichard, A. Gazzinelli, W. N. Grant, B. A. Boatin, J. S. McCarthy & M.G. Basanez, "A research agenda for helminth diseases of humans: the problem of helminthiases", PLoS neglected tropical diseases **6** (2012) 1582. https://doi.org/10.1371/journal.pntd.0001582.

[10] R. Tyagi, C. A. Bulman, F. Cho-Ngwa, C. Fischer, C. Marcellino, M. R. Arkin, J. H. McKerrow, C. W. McNamara, M. Mahoney, N. Tricoche et al., "An integrated approach to identify new antifilarial leads to treat river blindness, a neglected tropical disease", Pathogens **10** (2021) 71. https://doi.org/10.3390/pathogens10010071.

[11] A. Plaisier, G. Van Oortmarssen, J. Remme & J. Habbema, "The reproductive lifespan of onchocerca volvulus in west african savanna", Acta tropica **48** (1991) 271. https://doi.org/10.1016/0001-706X(91)90015-C.

[12] W. S. Alley, G. J. Van Oortmarssen, B. A. Boatin, N. J. Nagelkerke, A. P. Plaisier, J. H. Remme, J. Lazdins, G. J. Borsboom & J. D. F. Habbema, "Macrofilaricides and onchocerciasis control, mathematical modelling of the prospects for elimination", BMC Public health **1** (2020) 12. https://doi.org/10.1186/1471-2458-1-12.

[13] P. Milton, J. I. Hamley, M. Walker & M.-G. Basa´nez, "Moxidectin: an oral treatment for human onchocerciasis", Expert Review of Anti-Infective Therapy **18** (2020) 1067. https://doi.org/10.1080/14787210.2020.1792772.

[14] N. Mutono, M.G. Basanez, A. James, W. A. Stolk, A. Makori, T. N. Kimani, T. D. Hollingsworth, A. Vasconcelos, M. A. Dixon, S. J. de Vlas et al., "Elimination of transmission of onchocerciasis (river blindness) with long-term ivermectin mass drug administration with or without vector control in sub-saharan Africa: a systematic review and metaanalysis", The Lancet Global Health **12** (2024) 771. https://doi.org/10.1016/S2214-109X(24)00043-3.

[15] I. C. Oguoma and T. M. Acho, "Mathematical modelling of the spread and control of onchocerciasis in tropical countries: case study in Nigeria", Abstract and Applied Analysis **2014** (2014) 631658. https://doi.org/10.1155/2014/631658.

[16] E. Omondi, F. Nyabadza & R. Smith, "Modelling the impact of mass administration of ivermectin in the treatment of onchocerciasis (river blindness)", Cogent Mathematics & Statistics **5** (2018) 1429700. https://doi.org/10.1080/23311835.2018.1429700.

[17] K. Adeyemo, "Local stability analysis of onchocerciasis transmission dynamics with nonlinear incidence functions in two interacting populations", European Journal of Mathematical Analysis **3** (2023) 22. https://doi.org/10.28924/ada/ma.3.22.

[18] M. Konlan, B. Abassawah Danquah, E. Okyere, S. Osman, J. Amenyo Kessie & E. Kobina Donkoh, "Global stability analysis and modelling onchocerciasis transmission dynamics with control measures", Infection Ecology & Epidemiology **14** (2024) 11. https://doi.org/10.1080/20008686.2024.2347941.

[19] E. O. Omondi, F. Nyabadza, E. Bonyah & K. Badu, "Modeling the infection dynamics of onchocerciasis and its treatment", Journal of Biological Systems **25** (2017) 247. https://doi.org/10.1142/S0218339017500139.

[20] E. O. Omondi, T. O. Orwa & F. Nyabadza, "Application of optimal control to the onchocerciasis transmission model with treatment", Mathematical biosciences **297** (2018) 43. https://doi.org/10.1016/j.mbs.2017.11.009.

[21] M. G. Basa´nez, M. Walker, H. Turner, L. Co ˜ ffeng, S. De Vlas & W. Stolk, "River blindness: mathematical models for control and elimination", Advances in parasitology **94** (2016) 247. https://doi.org/10.1016/bs.apar.2016.08.003.

[22] M. Walker, W. A. Stolk, M. A. Dixon, C. Bottomley, L. Diawara, M. O. Traore, S. J. De Vlas & M.G. Bas anez, "Modelling the elimination of river blindness using long-term epidemiological and programmatic data from mali and senegal", Epidemics **18** (2017) 4. https://doi.org/10.1016/j.epidem.2017.02.005.

[23] I. Tirados, E. Thomsen, E. Worrall, L. Koala, T. T. Melachio & M.-G. Basa´nez, "Vector control and entomological capacity for onchocerciasis elimination", Trends in parasitology **38** (2022) 591. https://doi.org/10.1016/j.pt.2022.03.003.

[24] M. Saeedian, M. Khalighi, N. Azimi-Tafreshi, G. Jafari & M. Ausloos, "Memory effects on epidemic evolution: The susceptible-infected recovered epidemic model", Physical Review E **95** (2017) 022409. https://doi.org/10.1103/PhysRevE.95.022409.

[25] A. S. Shaikh, I. N. Shaikh & K. S. Nisar, "A mathematical model of covid-19 using fractional derivative: outbreak in india with dynamics of transmission and control", Advances in Difference Equations **2020** (2020) 373. https://link.springer.com/article/10.1186/s13662-020-02834-3.

[26] S. E. Fadugba, "Solution of fractional order equations in the domain of the mellin transform", Journal of the Nigerian Society of Physical Sciences **5** (2023) 138. https://doi.org/10.46481/jnsps.2019.31.

[27] R. Agarwal, P. Airan & R. P. Agarwal, "Exploring the landscape of fractional-order models in epidemiology: A comparative simulation study." Axioms **13** (2024) 13080545. https://doi.org/10.3390/axioms13080545.

[28] M. Vellappandi, P. Kumar & V. Govindaraj, "Role of fractional derivatives in the mathematical modeling of the transmission of chlamydia in the united states from 1989 to 2019", Nonlinear Dynamics **111** (2023) 4915. https://doi.org/10.1007/s11071-022-08073-3.

[29] K. S. Nisar, M. Farman, M. Abdel-Aty & J. Cao, "A review on epidemic models in sight of fractional calculus", Alexandria Engineering Journal **75** (2023) 81. https://doi.org/10.1016/j.aej.2023.05.071.

[30] P. Kumar, A. Kumar, S. Kumar & D. Baleanu, "A fractional order co-infection model between malaria and filariasis epidemic", Arab Journal of Basic and Applied Sciences **31** (2024) 132. https://doi.org/10.1016/j.aej.2023.05.071.

[31] D. Baleanu, H. Mohammadi & S. Rezapour, "A fractional differential equation model for the covid-19 transmission by using the caputo–fabrizio derivative", Advances in difference equations **2020** (2020) 299. https://doi.org/10.1016/j.aej.2023.05.071.

[32] J. Biazar, "Solution of the epidemic model by adomian decomposition method", Applied Mathematics and Computation **173** (2006) 1101. https://doi.org/10.1016/j.amc.2005.04.036.

[33] K. Diethelm and N. J. Ford, "Analysis of fractional differential equations", Journal of Mathematical Analysis and Applications **265** (2002) 229. https://doi.org/10.1006/jmaa.2000.7194.

[34] M. Ma, D. Baleanu, Y. S. Gasimov & X. J. Yang, "New results for multidimensional diffusion equations in fractal dimensional space", Rom. J. Phys. **61** (2016) 784. https://doi.org/10.1006/jmaa.2000.7194.

[35] J. C. Blackwood & L. M. Childs, "An introduction to compartmental modeling for the budding infectious disease modeler", Letters in Biomathematics **5** (2018) 195. https://doi.org/10.30707/LiB5.1Blackwood.

[36] A. O. Yunus & M. O. Olayiwola, "The analysis of a novel covid-19 model with the fractional-order incorporating the impact of the vaccination campaign in nigeria via the laplace-adomian decomposition method", Journal of the Nigerian Society of Physical Sciences **6** (2024) 1830. https://doi.org/10.46481/jnsps.2024.1830.

[37] D. Baleanu, F. A. Ghassabzade, J. J. Nieto & A. Jajarmi, "On a new and generalized fractional model for a real cholera outbreak", Alexandria Engineering Journal **61** (2022) 9175. https://doi.org/10.1016/j.aej.2022.02.054.

[38] A. I. K. Butt, "Atangana-baleanu fractional dynamics of predictive whooping cough model with optimal control analysis", Symmetry **15** (2023) 1773. https://doi.org/10.3390/sym15091773.

[39] M. O. Adewole, T. S. Faniran, F. A. Abdullah & M. K. Ali, "Covid-19 dynamics and immune response: Linking within-host and between-hostdynamics", Chaos, Solitons & Fractals **173** (2023) 113722. https://doi.org/10.1016/j.chaos.2023.113722.

[40] A. Atangana and R. T. Alqahtani, "Modelling the spread of river blindness disease via the caputo fractional derivative and the betaderivative", Entropy **18** (2016) 40. https://doi.org/10.3390/e18020040.

[41] A. A. Onifade, P. O. Odeniran, I. O. Ademola, A. Yusuf & S. S. Musa, "Modeling the dynamics of onchocerca volvulus with the impact of environmental factors on blackfly breeding sites", Scientific African **25** (2024) 02272. https://doi.org/10.1016/j.sciaf.2024.e02272.

[42] F. E. Guma, O. M. Badawy, M. Berir & M. A. Abdoon, "Numerical analysis of fractional-order dynamic dengue disease epidemic in sudan", Journal of the Nigerian Society of Physical Sciences **5** (2023) 1464. https://doi.org/10.46481/jnsps.2023.1464.

[43] P. Kumar, S. Kumar, B. S. Alkahtani & S. S. Alzaid, "A mathematical model for simulating the spread of infectious disease using the caputo-fabrizio fractional-order operator", AIMS Mathematics **9** (2024) 30864. https://doi.org/10.3934/math.20241490.

[44] M. Caputo and M. Fabrizio, "A new definition of fractional derivative without singular kernel", Progress in Fractional Differentiation & Applications **1** (2024) 73. https://doi.org/10.12785/pfda/010201.

[45] D. Baleanu, A. Mousalou & S. Rezapour, "On the existence of solutions for some infinite coefficient-symmetric caputo-fabrizio fractional integrodifferential equations", Boundary Value Problems **2017** (2017)1. https://doi.org/10.1186/s13661-017-0867-9.

[46] D. K. Almutairi, M. A. Abdoon, S. Y. M. Salih, S. A. Elsamani, F. E. Guma & M. Berir, "Modeling and analysis of a fractional visceral leishmaniosis with caputo and caputo–fabrizio derivatives", Journal of the Nigerian Society of Physical Sciences **5** (2023) 1453. https://doi.org/10.46481/jnsps.2023.1453.

[47] A. Shaikh, A. Tassaddiq, K. S. Nisar & D. Baleanu, "Analysis of differential equations involving caputo–fabrizio fractional operator and its applications to reaction–diffusion equations", Advances in Difference Equations **2019** (2019) 1. https://doi.org/10.1186/s13662-019-2115-3.

[48] D. Baleanu, S. Rezapour & Z. Saberpour, "On fractional integrodifferential inclusions via the extended fractional caputo–fabrizio derivation", Boundary Value Problems **2019** (2019) 1. https://doi.org/10.1186/s13661-019-1194-0.

[49] E. J. Moore, S. Sirisubtawee & S. Koonprasert, "A caputo– fabrizio fractional differential equation model for HIV/AIDS with treatment compartment", Advances in Difference Equations **2019** (2019) 21389. https://doi.org/10.1186/s13662-019-2138-9.

[50] A. S. Alshehry, H. Yasmin, A. A. Khammash & R. Shah, "Numerical analysis of dengue transmission model using caputo–fabrizio fractional derivative", Open Physics **22** (2024) 0169. https://doi.org/10.1515/phys-2023-0169.

[51] Y. M. Chu, M. F. Khan, S. Ullah, S. A. A. Shah, M. Farooq & M. bin Mamat, "Mathematical assessment of a fractional-order vector– host disease model with the caputo–fabrizio derivative", Mathematical Methods in the Applied Sciences **22** (2024) 0169. https://doi.org/10.1002/mma.8507.

[52] K. M. Owolabi and A. Atangana, "Analysis and application of new fractional adams–bashforth scheme with caputo–fabrizio derivative", Chaos, Solitons & Fractals **105** (2017) 111. https://doi.org/10.1016/j.chaos.2017.10.020.

[53] A. I. K. Butt, M. Imran, K. Azeem, T. Ismaeel & B. A. McKinney, "Analyzing hiv/aids dynamics with a novel caputofabrizio fractional order model and optimal control measures", PloS one **19** (2019) 0315850. https://doi.org/10.1371/journal.pone.0315850.

[54] T. R. Nandi, A. K. Saha & S. Roy, "Analysis of a fractional order epidemiological model for tuberculosis transmission with vaccination and reinfection", Scientific Reports **14** (2024) 28290. https://doi.org/10.1038/s41598-024-73392-x.

[55] J. Losada and J. J. Nieto, "Properties of a new fractional derivative without singular kernel", Progr. Fract. Differ. Appl **1** (2015) 87. https://doi.org/10.12785/pfda/010202.

[56] T. Abdeljawad and D. Baleanu, "On fractional derivatives with exponential kernel and their discrete versions", Reports on Mathematical Physics **80** (2017) 11. https://doi.org/10.1016/S0034-4877(17)30059-9.

[57] H. Yang, S. Qaisar, A. Munir & M. Naeem, "New inequalities via caputo-fabrizio integral operator with applications", Aims Math **8** (2023) 19391. https://doi.org/10.3934/math.2023989.

[58] M. Khalighi, G. Sommeria-Klein, D. Gonze, K. Faust & L. Lahti, "Quantifying the impact of ecological memory on the dynamics of interacting communities", PLoS computational biology **18** (2022) 1009396. https://doi.org/10.1371/journal.pcbi.1009396.

[59] H. F. Huo, R. Chen & X. Y. Wang, "Modelling and stability of hiv/aids epidemic model with treatment", Applied Mathematical Modelling **40** (2016) 6550. https://doi.org/10.1016/j.apm.2016.01.054.

[60] P. Van den Driessche & J. Watmough, "Reproduction numbers and subthreshold endemic equilibria for compartmental models of disease transmission", Mathematical biosciences **180** (2002) 29. https://doi.org/10.1016/S0025-5564(02)00108-6.

[61] M. Bani-Yaghoub, R. Gautam, Z. Shuai, P. Van Den Driessche & R. Ivanek, "Reproduction numbers for infections with freeliving pathogens growing in the environment", Journal of biological dynamics **6** (2012) 923. https://doi.org/10.1080/17513758.2012.693206.

[62] H. Li, J. Cheng, H.-B. Li & S.-M. Zhong, "Stability analysis of a fractional-order linear system described by the caputo–fabrizio derivative", Mathematics **7** (2019) 200. https://doi.org/10.3390/math7020200.

[63] U. T. Mustapha, Y. U. Ahmad, A. Yusuf, S. Qureshi & S. S. Musa, "Transmission dynamics of an age-structured hepatitis-b infection with differential infectivity", Bulletin of Biomathematics **1** (2023) 124. https://doi.org/10.59292/bulletinbiomath.2023007.

[64] S. W. Teklu, "Mathematical analysis of the transmission dynamics of covid-19 infection in the presence of intervention strategies", Journal of Biological Dynamics **16** (2022) 640. https://doi.org/10.1080/17513758.2022.2111469.

[65] S. Ajao, I. Olopade, T. Akinwumi, S. Adewale & A. Adesanya, "Under-

standing the transmission dynamics and control of hiv infection: A mathematical model approach", Journal of the Nigerian Society of Physical Sciences **5** (2023) 1389. https://doi.org/10.46481/jnsps.2023.1389.

[66] Z. H. Shen, Y. M. Chu, M. A. Khan, S. Muhammad, O. A. Al-Hartomy, & M. Higazy, "Mathematical modeling and optimal control of the covid-19 dynamics", Results in Physics **31** (2021) 105028. https://doi.org/10.1016/j.rinp.2021.105028.

[67] E. A. Nwaibeh and M. K. Ali, "Covid-19 dynamic modeling of immune variability and multistage vaccination strategies: a case study in malaysia", Infectious Disease Modelling **10** (2025) 011. https://doi.org/10.1016/j.idm.2024.12.011.

[68] D. Gerbet & K. Robenack, "Application of Lasalle's invariance principle "on polynomial differential equations using quantifier elimination", IEEE Transactions on Automatic Control **67** (2025) 3590. https://doi.org/10.1109/TAC.2021.3103887.

[69] C. F. Lee, C. Y. Weng & C. Y. Kao, "Reversible data hiding using Lagrange interpolation for prediction-error expansion embedding", Soft Computing **23** (2019) 9719. https://doi.org/10.1007/s00500-018-3537-7.

[70] Ghana Health Services, "Two-year strategic plan for integrated neglected tropical diseases control in ghana 2007–2008", Ghana Health Services, 2016. http://www.moh-ghana.org/UploadFiles/Publications/Plan%20for%20Pro-Poor%20Diseases120506091943.pdf.

[71] D. Chicco, M. J. Warrens & G. Jurman, "The coefficient of determination R-squared is more informative than smape, mae, mape, mse and rmse in regression analysis evaluation", Peerj computer science **7** (2021) 623. https://doi.org/10.7717/peerj-cs.623.

[72] A. D. W. Sumari, D. S. Charlinawati & Y. Ariyanto, "A simple approach using statistical-based machine learning to predict the weapon system operational readiness", in Proceedings of the International Conference on Data Science and Official Statistics **2021** (2021) 343. https://doi.org/10.34123/icdsos.v2021i1.58

[73] Y. S. Lee and L. I. Tong, "Forecasting energy consumption using a grey model improved by incorporating genetic programming", Energy conversion and Management **252** (2011) 147. https://doi.org/10.1016/j.enconman.2010.06.053.

[74] A. Hopkins and B. A. Boatin, "Onchocerciasis:water and sanitationrelated diseases and the environment: challenges, interventions, and preventive measures", Scientific Reports **2011** (2011) 133. https://doi.org/10.1002/9781118148594.ch8.

[75] I. Onwubuya, G. Nkem, N. Tindi & C. Madubueze, "Optimal control analysis of onchocerciasis transmission model", International Journal of Mathematical Analysis and Modelling **6** (2023) 1. https://tnsmb.org/journal/index.php/ijmam/article/view/78.

[76] J. C. Nguyen, M. M. E. Murphy, T. B. Nutman, R. C. Neafie, L. S. Maturo, D. S. Burke & C. G. W. Turiansky, "Cutaneous onchocerciasis in an american traveler", International journal of dermatology **44** (2005) 125. https://doi.org/10.1111/j.1365-4632.2004.02203.x.

[77] A. Hassan and N. Shaban, "Onchocerciasis dynamics: modelling the effects of treatment, education and vector control", Journal of Biological Dynamics **14** (2020) 245. https://doi.org/10.1080/17513758.2020.1745306.

[78] N. Chitnis, J. M. Hyman & J. M. Cushing, "Determining important parameters in the spread of malaria through the sensitivity analysis of a mathematical model", Bulletin of mathematical biology **14** (2020) 245. https://doi.org/10.1007/s11538-008-9299-0.